Cervical Cancer Detection From Cervix Image Using Pap Smear Imaging Through CNN

by

Mazedul Haque Bhuiyan
15201035
FaribaTabassum
15201038
Umme Bushra
15201034
Md.Mahbub Rahman Shwon
15201044

A thesis submitted to the Department of Computer Science and Engineering
in partial fulfillment of the requirements for the degree of
B.Sc. in Computer Science

Department of Computer Science and Engineering
Brac University
April 2020

Declaration

It is hereby declared that

1. The thesis submitted is my/our own original work while completing degree at Brac University.
2. The thesis does not contain material previously published or written by a third party, except where this is appropriately cited through full and accurate referencing.
3. The thesis does not contain material which has been accepted, or submitted, for any other degree or diploma at a university or other institution.
4. We have acknowledged all main sources of help.

Student's Full Name & Signature:

Mazedul Haque Bhuiyan
15201035

Fariba Tabassum
15201038

Umme Bushra
15201034

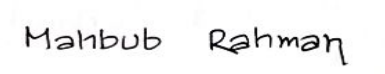

Md.Mahbub Rahman Shwon
15201044

Approval

The thesis/project titled "Cervical Cancer Detection From Cervix Image Through Deep Belief Network" submitted by

1. Mazedul Haque Bhuiyan (15201035)
2. Fariba Tabassum (15201038)
3. Umme Bushra (15201034)
4. Md.Mahbub Rahman Shwon (15201044)

Of Summer, 2020 has been accepted as satisfactory in partial fulfillment of the requirement for the degree of B.Sc. in Computer Science on April 19, 2020.

Examining Committee:

Supervisor:
(Member)

Md. Golam Rabiul Alam
Associate Professor
Department of Computer Science and Engineering
Brac University

Head of Department:
(Chair)

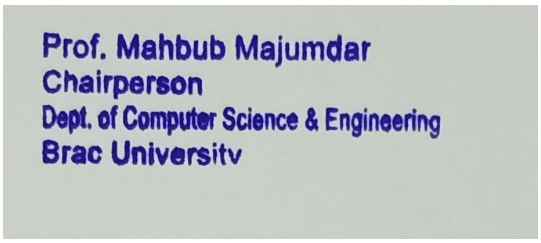

Mahbubul Alam Majumdar
Professor and Chairperson
Department of Computer Science and Engineering
Brac University

Ethics Statement (Optional)

The intellectual content of submitted manuscripts is evaluated is evaluated regardless of race, gender, sexual orientation, age, disability, religion, ethnicity, political philosophy of the authors.

All manuscripts should be treated as confidential documents. They must not be shown to anyone without the permission of the editor. Managers and editorial staff should not disclose information about the manuscript submitted to anyone except the author, reviewers and potential reviewers.

Unpublished data contained in the submitted manuscript must not be used by editors or reviewers in their own research without the explicit consent of the author.

The editor of Communication Organization decides on the publication of submitted articles. The editor is guided by the Editorial Committee's policy, taking into account the legal obligations regarding defamation, copyrights and plagiarism. The editor can share the decision with other members of the Editorial Board or with reviewers. In the event of an appeal of the decision of the Reading Committee, the editor may solicit two new reviewers.

Abstract

Uterine cervical cancer is the second most regular gynecological harm around the world. The appraisal of the degree of sickness is fundamental for arranging ideal treatment. Imaging procedures are progressively utilized in the pre-treatment work-up of cervical malignancy[22]. Presently, MRI for the neighborhood degree of sickness assessment and PET-check for removed ailment appraisal is considered as first-line procedures. In any case, over the most recent couple of years, ultrasound has picked up consideration as an imaging system for assessing ladies with cervical cancer.In this paper, we will take a shot at the advancement of a profound conviction system to order ultrasound pictures of the cervical cells to recognize cervical malignant growth.

This postulation talks about the depiction of examples of single pap-smear cells from a current database set up at Herlev University Hospital. Wellbeing, the apparatus ought to be utilized before disease improvement to distinguish pre-dangerous cells in the uterine cervix[16]. For the separation among ordinary and unusual cells, open cell qualities, for example, area, position, and splendor of the core and cytoplasm are utilized. The exhibition of the classifier is determined on the rate total blunder but on the other hand is tried on the recurrence of bogus negative and bogus positive mistakes. The point is to support the all out mistake instead of the outcomes acquired already.

A detailed overview of Herlev University Hospital's latest pap- data prepares a new comparison platform Papsmear for publishing on Twitter. The papsmear collection consists of 917 experiments on 7 separate types of normal and irregular cells spread unequally. Every sample is represented by 20 characteristics. The average performance of the tested classifiers indicates no substantial change in earlier tests, but similar results are obtained using very basic methods.

Keywords: Cervical Cancer; Deep Learning; Cervix; Prediction; PCA; t-SNE; AUC-ROC Curve; XGBooster; SVM; CNN;

Acknowledgement

Firstly, all praise to the Great Allah for whom our thesis have been completed without any major interruption.
Secondly, to our co-advisor Md. Golam Rabiul Alam sir for his kind support and advice in our work. He helped us whenever we needed help.
Thirdly, the whole judging panel of Computer Science & Engineering department of BRAC University. All the reviews they gave helped us a lot in our later works.
And finally to our parents without their throughout sup-port it may not be possible. With their kind support and prayer we are now on the verge of our graduation.

Table of Contents

List of Figures

Nomenclature

The next list describes several symbols & abbreviation that will be later used within the body of the document

AUC Area Under the Curve

CNN Convolutional Neural Network

PCA Principle Component Analysis

ROC Receiver Operating Characteristic

SVM Support Vector Machine

$t - SNE$ T-distributed Stochastic Neighbor Embedding

XGB XGBoost Algorithm

Chapter 1

Introduction

1.1 Thoughts behind the Cervical Cancer Detection Model

The cervical disease is the second most gynecological danger on the planet. Cervical malignant growth influences the passage of the belly. There are diverse screening strategies utilized for identifying cervical malignant growth [15]. The Pap smear test or fluid cytology-based (LCB) tests are finished by physically gathering the phones of the cervix. From the previous not many decades, broad research has been committed to the formation of PC helped to peruse frameworks dependent on computerized picture examination techniques. Imaging procedures are progressively utilized in the pre-treatment workup of cervical malignant growth. A profound conviction organize is utilized to perceive, bunch and creates pictures. A profound conviction system can be characterized as a heap of limited Boltzmann machines, in which each layer speaks with both the past and consequent layers[10]. The hubs of any single layer don't speak with each layer horizontally. The complete number of hubs or layers is subject to the number of information pictures utilized. There are numerous layers of shrouded units, each layer has a twofold job: it fills in as the concealed layer to hubs that precede it, and as the info layer to the hubs that come after. The stack closes with a SoftMax layer to make a classifier, or it might essentially help bunch unlabeled information in a solo learning situation.

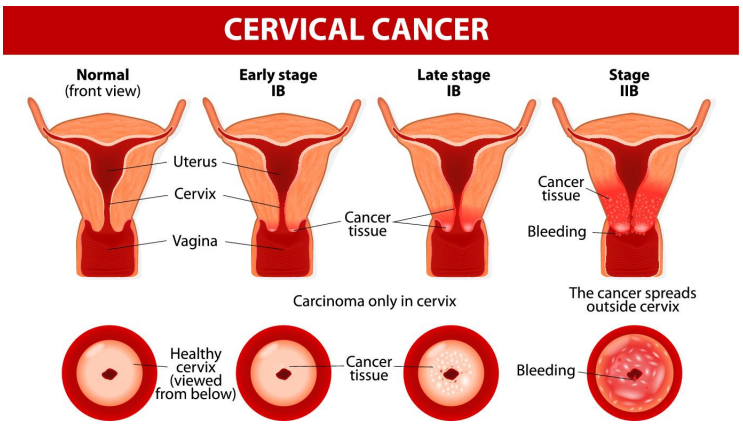

Figure 1.1: Cervical Cancer Stages

1.2 Aims and Objectives

The objective is two-fold

- Distributing a solid example database of pap-smear information used to check and assess different characterization techniques
- Evaluating the result by analyzing the normal and abnormal cervix cell using these data by implementing the DBN(Deep Belief Network) & contrasting the findings with previous classifiers based on the data

1.3 History of Cervical Cancer

Cervical malignant growth is a disease that starts from the cervix. It is ascribed to the unpredictable advancement of cells that are fit for entering or growing to different regions of the body. No signs are normally observed right off the bat. Later signs during sex can incorporate sporadic vaginal dying, stomach inconvenience or sickness. Albeit after-sex draining may not be not kidding, it might likewise propose cervical disease.
Human papillomavirus disease (HPV) influences more than 90 percent of cases; be that as it may, most ladies with HPV contamination's don't create cervical malignant growth. Other hazard factors incorporate liquor, a poor resistant framework, anti-conception medication drugs, beginning pubescence at a youthful age and having different sexual accomplices, even though they are less huge.
Cervical malignant growth, for the most part, advances from precancerous adjustments more than 10 to 20 years. Around 90 percent of instances of a cervical malignant growth are squamous cell carcinomas, 10 percent are adenocarcinoma, and a restricted rate are different sorts. Determination, for the most part, requires cervical screening followed by a biopsy. Clinical imaging is regularly performed to decide if the disease has progressed or has not.
Acting in the mid-twentieth century, disease transmission experts saw that cervical malignancy acted like an explicitly transmitted illness. Listed Summary:

- It was accounted for that cervical malignant growth is far reaching among female sex laborers.
- Among nuns, it was exceptional yet for the individuals who had been explicitly drawn in since they joined the religious circle.
- Men whose first spouses had passed on from cervical malignancy turned out to increasingly visit in the subsequent wives.
- This was uncommon among individuals of Jewish plummet.
- In 1935, Syverton and Berry found that RPV (Rabbit Papillomavirus) and hare skin malignant growth were connected.

Those verifiable discoveries demonstrated that an explicitly transmitted operator could cause cervical malignant growth. Unique work during the 1940s and 1950s connected smegma to cervical disease (e.g., Heins et al., 1958). In the sixties and seventies, it was accepted that herpes simplex infection contamination was the reason

for the ailment. In outline, HSV was viewed as a potential trigger since it is known to live in the female regenerative tract, to be explicitly transmitted in a way reliable with set up chance factors, for example, wantonness and low financial status.
Numerous dangerous malignancies, including Burkitt's lymphoma, Nasopharyngeal carcinoma, Marek's infection, and Lucké renal adenocarcinoma, likewise included herpes infections. HSV has been recovered from cells of the cervical tumor.
A portrayal by electron microscopy of human papillomavirus (HPV) was given in 1949, and HPV-DNA was recognized in 1963. It was not until the 1980s that HPV was distinguished in cervical malignant growth tissues. HPV has been seen as ensnared in about each cervical malignancy since. The regular viral subtypes influenced are HPV 16, 18, 31, 45 and others. All through the examination began in the mid-1980s, specialists at the Georgetown University Medical Center, the University of Rochester, the University of Queensland in Australia and the U.S. built up the HPV immunization pair. National Cancer Institute. The United States, in 2006 The principal preventive HPV antibody, sold by Merck and Co. under the exchange name Gardasil, was affirmed by the Food and Drug Administration (FDA).

1.4 Problem Statement

A full rundown of the information assortment expected to distribute the most recent pap-smear information for benchmark testing. The definition should be an independent part of a straightforward World Wide Web discharge. It is critical to characterize all info includes independently, to express their physical root. Photographs are to be utilized for putting away end-clients. A full definition regularly incorporates a synopsis of the outcomes, portraying the various kinds of cells utilized in the word pap-smear[15]. Inside this examination, new transductive strategies are acquainted with pap-smear recognition by reinforcing Martin's prior results(2003).

Chapter 2

Literature Review

In recent years, Deep learning and PC vision have demonstrated success in the human services area for characterization or division of clinical pictures [26]. Late endeavors utilizing profound adapting for the most part either use move learning with models pre-prepared on ImageNet or duplicate the design of these models and train them without any preparation. One ongoing endeavor at cervical disease arrangement consolidated picture highlights from the last completely associated layer of pre-prepared AlexNet with organic highlights extricated from a Pap smear to make the expectation [20]. Besides, Another gathering utilized highlights processed from pictures of cells from a cervix biopsy as a contribution to a feed-forward neural system to anticipate the nearness of malignant growth. Other manual highlights from a Pap smear, for example, Gray level, wavelet, and Gray level co-event network have been utilized for malignant growth locations. Profound learning has likewise been utilized for different kinds of malignant growth identification. A convolutional neural system (CNN) following OxfordNet's structure was utilized to recognize mammographic injuries. [14]A CNN with parameters pre-prepared on a comparative dataset was likewise used to separate between mammographic sores and sores. An ongoing paper from a gathering of Stanford analysts has energized the clinical network and uses a pre-prepared Inception-v3 model and progressive calculation to characterize distinctive skin malignancies with results practically identical to master dermatologists [17]. Another examination dissected colonoscopy video film and utilized CNN to register picture highlights which were afterward used to anticipate the bounding boxes for various polyps.

Chapter 3

Proposed Model

3.1 Dataset Description

A chronicle of single pap-smear cell pictures is acquired at Herlev University Hospital, attributable to a huge assortment of glass slides. Proficient cytotechnicians utilized a 0.201m/pixel goal magnifying lens to catch single-cell optical pictures. A short time later, every cell picture is physically assembled into the 7 diverse cell structures recorded in figure 2.4. Specific cytotechnicians do the classification frequently for confirmation [28]. If the confirmation is unfavorable then the image will be discarded. The seven definitions are similar to those that are used for standard manual diagnosis.

Normal - 242 cells

. 1 Superficial squamous epithelial, 74 cells.

. 2 Intermediate squamous epithelial, 70 cells

. 3 Columnar epithelial, 98 cells.

Abnormal - 675 cells

. 4 Mild squamous non-keratinizing dysplasia, 182 cells.

. 5 Moderate squamous non-keratinizing dysplasia, 146 cells.

. 6 Severe squamous non-keratinizing dysplasia, 197 cells.

. 7 Squamous cell carcinoma in situ intermediate, 150 cells.

Figure 3.1: The 7 different pap-smear classes

3.2 Working Plan

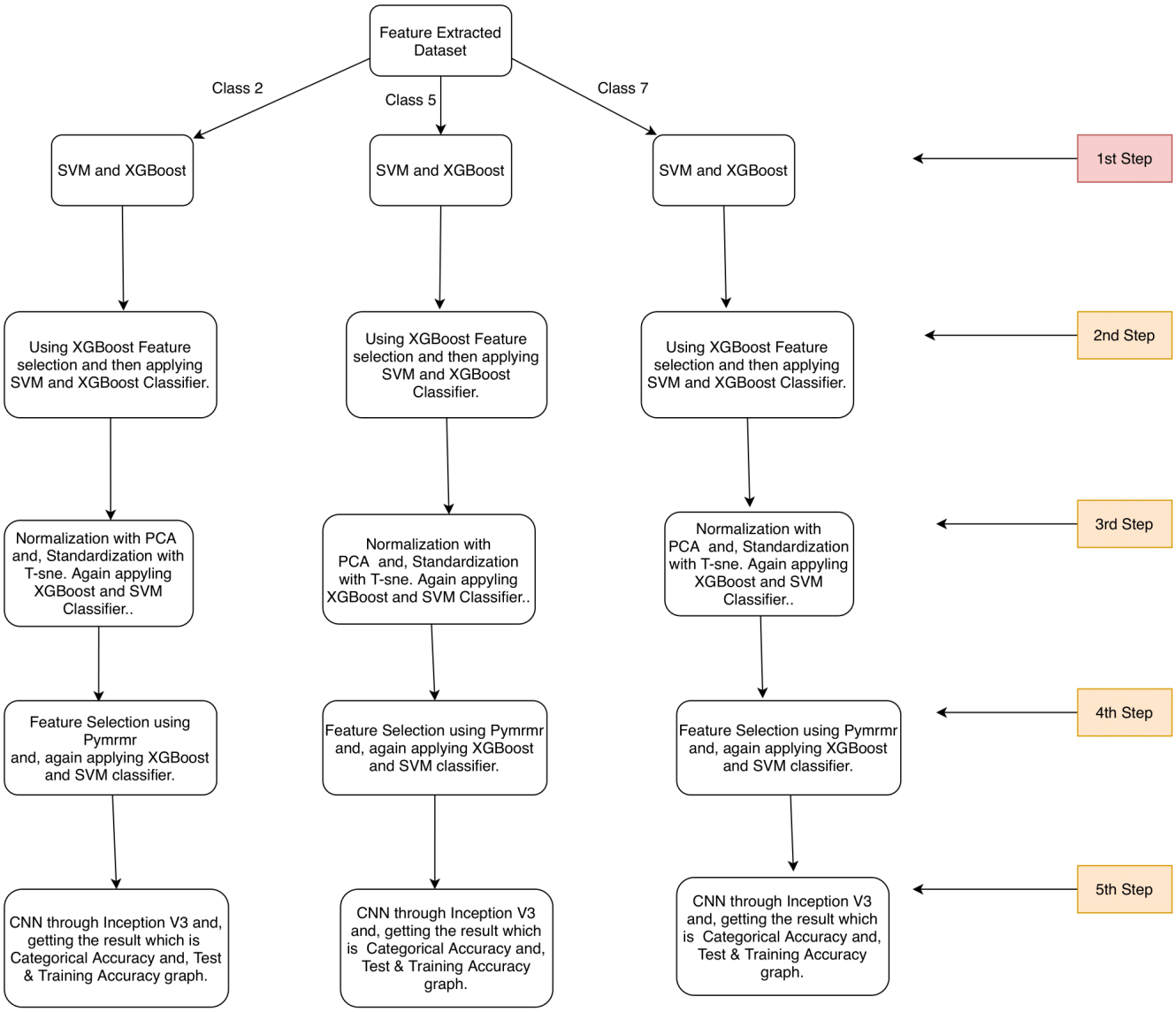

Figure 3.2: Working Plan

3.3 Algorithm Description

3.3.1 PCA: Principle Component Analysis

The Principal Component Analysis (PCA) is a factual method that utilizes asymmetrical change to decipher a progression of estimations of hypothetically related factors into an assortment of estimations of directly uncorrelated factors called key parts. This change is characterized so that the primary fundamental part has the best conceivable fluctuation, and every successor segment, thus, has the best conceivable difference under the imperative of being symmetrical to the former segments. The subsequent vectors (a direct blend of the factors and n perceptions) are an uncorrelated arrangement of symmetrical bases [13]. PCA is defenseless against the corresponding scaling of the first factors.

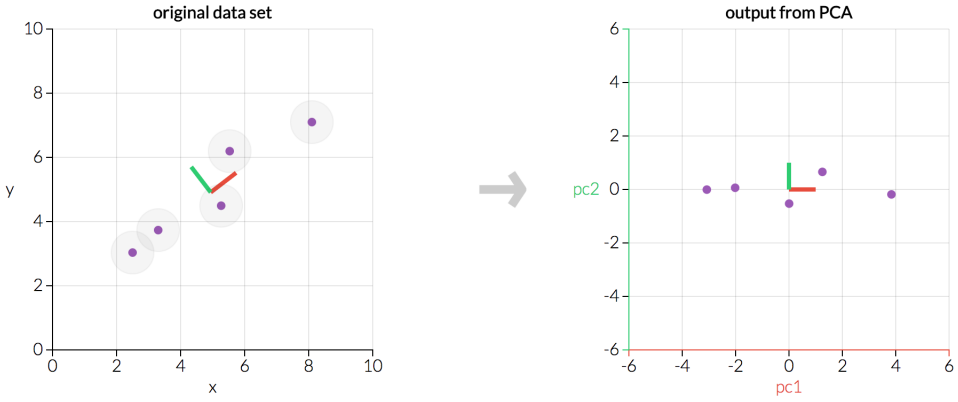

Figure 3.3: PCA Analysis

Karl Pearson found PCA in 1901 as a guess of the primary pivot hypothesis of mechanics; it was later grown freely and named during the 1930s by Harold Hotelling. Contingent upon the field of activity, it is regularly alluded to as the discrete Karhunen – Loève change (KLT) in signal handling, the Hotelling change into multivariate quality control, appropriate symmetrical disintegration (POD) in mechanical designing, particular worth deterioration (SVD) of X (Golub and Van Loan, 1983), singular worth decay (EVD) of XTX indirect variable based math, factor investigation (for a conversation of the contrasts among PCA and factor examination). Eckart – Young hypothesis (Harman, 1960), or observational symmetrical capacities (EOF) in meteorological material science, exact self-useful decay (Sirovich, 1987), experimental part examination (Lorenz, 1956), semi consonant modes (Brooks et al., 1988), clamor and vibration unearthly disintegration, and basic elements exact modular investigation.
PCA is chiefly utilized as an apparatus for exploratory information preparation and factual model structure [13]. This is likewise used to portray the developmental inlet and interpopulation relatedness. PCA might be accomplished by disintegrating an information covariance (or relationship) lattice by its worth, or by breaking down an information grid by a solitary worth, for the most part, after the first information has been standardized. - property's standardization comprises of mean focusing – subtracting - information esteem from the assessed mean of its segment with the goal that its numerical mean (normal) is 0. Besides normalizing the mean, certain

fields do as such with the fluctuation of every factor (to make it equivalent to 1); see Z-scores.

3.3.2 t-SNE: T-distributed Stochastic Neighbor Embedding

T-distributed Stochastic Neighbor Embedding (t-SNE) is a perception calculation created by Laurens van der Maaten and Geoffrey Hinton for AI [18]. This is an appropriate nonlinear dimensionality decrease strategy for installing high-dimensional information for perception in a few-dimensional, low-dimensional space. It shows every high-dimensional item from a few-dimensional point so that indistinguishable articles are demonstrated by neighboring focuses, and unique articles are displayed by high-likelihood far off focuses.

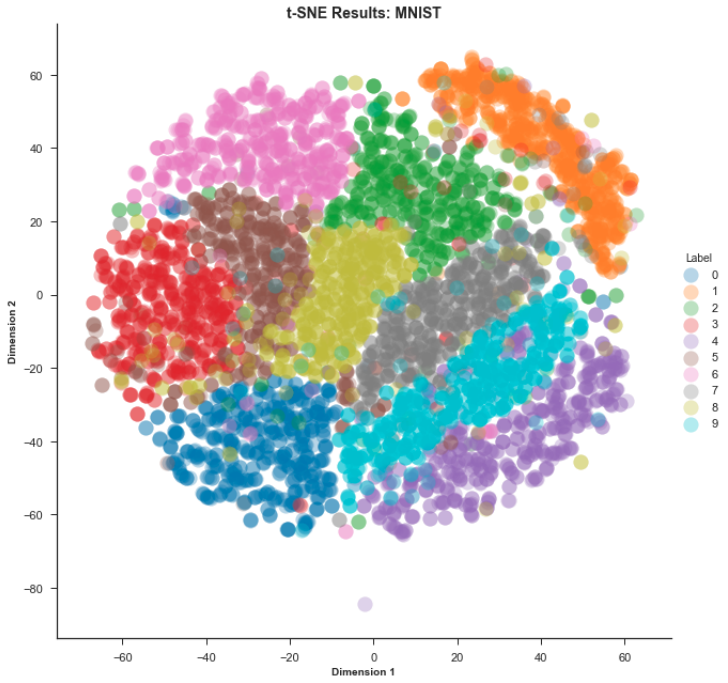

Figure 3.4: t-SNE Analysis

There are two key periods of the t-SNE calculation. To begin with, t-SNE constructs an appropriation of likelihood over sets of high-dimensional items in such a way, that indistinguishable articles are almost certain to be chosen while unique focuses have an extraordinarily low possibility of being picked [18]. Second, t-SNE decides a similar conveyance of likelihood over the focuses on the low-dimensional circle and limits the Kullback – Leibler difference (KL disparity) between the two circulations concerning the places of the focuses on the circle. Notice that while the first calculation utilizes the Euclidean separation between objects as the premise of its measurement of similarity, this can be changed if essential.
T-SNE has been utilized in a wide assortment of uses for perception, including data security testing, music examination, malignancy look into, bioinformatics, and biomedical sign preparing [18]. It is additionally utilized for imagining significant level portrayals that a counterfeit neural system knows.
Even though t-SNE plots now and again will, in general, speak to bunches, the picked parameterization will emphatically impact the visual groups, and hence an away

from the t-SNE parameters is required. Such "groups" can be appeared to try and show up in non-bunched information, and accordingly might be bogus discoveries. The intelligent investigation may along these lines be important to pick parameters and approve results. It has been demonstrated that t-is constantly ready to recoup well-groups and is approximating an essential technique for phantom bunching with various parameter decisions.

3.3.3 pymRMR

pymRMR gives the single-passage point technique pymrmr.mRMR(). The information ought to be given as of now discretized, as characterized in the first paper. This rendition of the calculation doesn't give discretization, uniquely in contrast to the first C code.
This technique requires 3 information parameters:

- The main parameter is a Pandas Data Frame containing the information dataset, discretized as characterized in the first paper. The lines of the dataset are different examples. The primary segment is the arrangement (target) variable for each example. The rest of the sections are the various factors (includes) that might be chosen by the calculation.

- The subsequent parameter is a string which characterizes the inner Feature Selection technique to use(defined in the first paper): potential qualities are "MIQ" or "MID"

- A third parameter is a whole number which characterizes the number of highlights that ought to be chosen by the calculation. The arrival worth might be a rundown containing the names of the picked highlights.

3.3.4 XGBooster

XGBoost is a Machine Learning calculation concentrated on a choice tree gathering that utilizes an inclination boosting framework [21]. Counterfeit neural systems seem to beat every single other design or framework when determining issues including unstructured information (pictures, content, and so on.). Be that as it may, choice tree-calculations are viewed as best right now with regards to little to medium organized.
XGBoost Algorithm was made by the University of Washington as an exploration venture. At the SIGKDD Conference in 2016, Tianqi Chen and Carlos Guestrin conveyed their paper and took the field of AI on the tempest. After its dispatch, this calculation has been acknowledged for winning a few Kaggle rivalries as well as the managing power behind the hood for some, bleeding-edge applications in the business. As an outcome, with 350 engineers and 3,600 commitments on GitHub, there is an enormous gathering of information researchers adding to XGBoost open-source ventures. The calculation separates itself in such regards as:

- An expansive assortment of uses: Can be utilized to take care of issues with relapse, arrangement, rating, and client characterized forecast.

- Portability: Smooth running on Windows, Linux, and OS X.

- Languages: Supports every single significant language of programming including C++, Python, R, Java, Scala, and Julia.
- Cloud Integration: Supports groups with AWS, Azure, and Yarn and works well with Flink, Spark, and different biological systems.

XGBoost Perfomance

XGBoost and Gradient Boosting Machines (GBMs) are both outfit tree strategies that utilization the inclination plunge engineering guideline of boosting frail students (CARTs by and large). XGBoost, in this way, expands on the base GBM engineering by refining structures and creating calculations [21].

- Parallelisation: XGBoost utilizes a parallelized usage to handle the technique for successive tree creation. It is conceivable as a result of the tradable idea of circles used to make base students; the external circle specifying a tree's leaf hubs, and the second internal circle estimating the highlights. Such circle settling limits parallelization, as the external circle, can not be begun without finishing the inward circle (all the more computationally requesting of the two). Along these lines, the request for circles is traded utilizing introduction through a worldwide hunt everything being equal and arranging to utilize simultaneous strings to amplify run time [3]. This progress builds the productivity of calculations by Offsetting any overhead parallelization in registering.
- Tree Pruning: The tree parting stop measure inside the GBM framework is insatiable, and depends on the split point's misfortune rule. XGBoost utilizes the parameter 'max profundity' as characterized first, rather than the criteria, and starts pruning trees in reverse. This 'profundity first' strategy incredibly upgrades computational effectiveness.
- Computer streamlining: This calculation was created to utilize PC assets proficiently. It is practiced by information on the reserve by assigning interior cradles to store slope insights in each string. Discretionary upgrades like out-of-center figuring boost usable circle space while taking care of gigantic information outlines that don't fit into memory.

Entropy

Entropy is a proportion of capriciousness and vulnerability of an informational collection. Entropy is commonly considered to decide how scattered an informational collection is [11]. The higher pace of entropy alludes to the vulnerability and more data required in these cases to improve consistency. One result is particularly sure when the entropy is zero.

$$Entropy(S) = \sum_{i=1}^{C} Pi \log_2 Pi \tag{3.1}$$

Where Pi is the extent of occasions in the informational index that takes the estimation of the objective trait, which has C various qualities. This likelihood measure

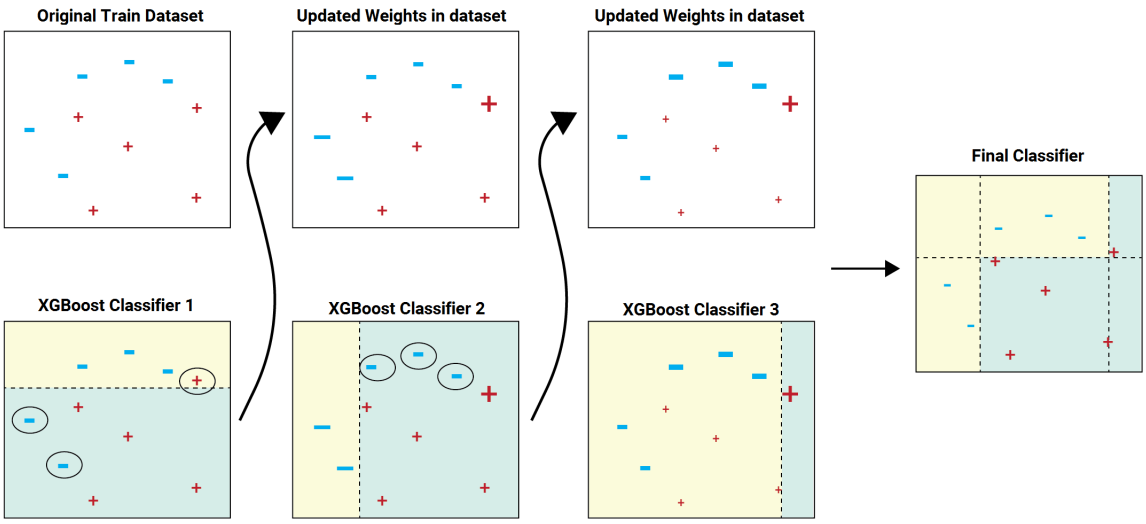

Figure 3.5: XGBoost Algorithm

gives us how dubious we are about the information. We utilize a log2 measure as this speaks to what number of bit we would need to determine what the class is of an arbitrary example.

Information Gain

Presently we need a quantitative method for parting the informational index by utilizing a specific trait. We can utilize a measure called Information Gain, which computes the decrease in entropy that would bring about parting the information on a property, A. Data Gain is a technique to choose the specific credit to be a choice hub of a choice tree [7].

$$Gain(S, A) = Entropy(S) - \sum_{v \epsilon A} \frac{S_v}{S} Entropy(S_v) \tag{3.2}$$

where v is an estimation of A, Sv is the subset of occasions of S where A takes the worth v and S is the number of occurrences With the assistance of this hub assessment system we can continue recursively through the subset we make until leaf hubs have been reached all through and all subsets are unadulterated with zero entropy. This is how a choice tree calculation works.

3.3.5 SVM: Support Vector Machine

Support machines (SVMs, additionally support-networks[1]) in AI are managed to learn models with related learning calculations that reproduce information utilized for order and relapse examination [4]. In light of an assortment of preparing models, every one of which is set apart as having a place with either of two classes, an SVM preparing calculation makes a model which allows new guides to either class, making it a non-probabilistic paired direct classifier (in spite of the fact that strategies, for example, Platt scaling exist to utilize SVM in the probabilistic arrangement).

An SVM model is a portrayal of the models as space focuses, mapped so as to recognize the models in various classifications by a basic separation that is as wide as could be expected under the circumstances. At that point, new occurrences are anticipated into a similar space and expected to have a place with a division relying upon the side of the void they failed to work out.
Notwithstanding performing direct arrangement, SVMs can productively play out a non-straight order utilizing what is known as the bit stunt, certainly mapping their contributions to high-dimensional element spaces. Where information is unlabeled, managed learning isn't attainable and an unaided learning strategy is required, which expects to locate a typical bunching of information into classes, and afterward maps new information to these built-up gatherings. The grouping support vector[2] calculation created by Hava Siegelmann and Vladimir Vapnik utilizes bolster vector measurements worked in the help vector framework calculation to order unlabeled information and is one of the most usually used bunching calculations in modern applications.

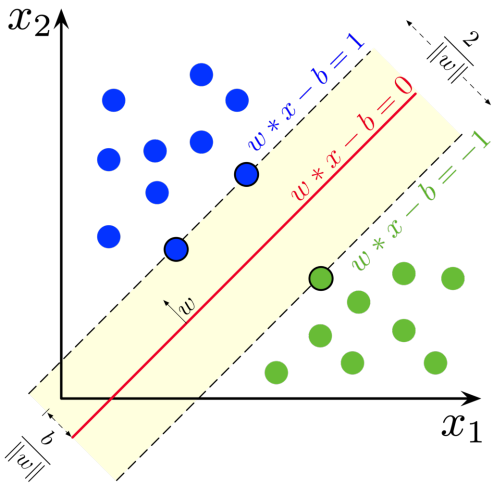

Figure 3.6: Support Vector Machine

SVMs can be utilized to address various certifiable issues:

- SVMs are helpful in arranging content and hypertext, as their utilization will incredibly diminish the requirement for marked preparing cases in both the customary inductive and transductive conditions. Numerous methodologies depend on vector bolster machines for the shallow semantic parsing.
- Even picture recognition can be accomplished by utilizing SVMs. Trial tests uncover that after just three or four rounds of direct surveys, SVMs arrive at extensively preferable hunt accuracy over ordinary inquiry advancement plans.
- Classification of satellite information utilizing controlled SVM, for example, SAR information.
- Hand-composed characters can be perceived by utilizing SVM.
- The SVM calculation has been ordinarily utilized in the studies of science and different subjects. They were utilized to distinguish suitably classified proteins for up to 90 percent of the mixes. Stage tests concentrated on SVM loads were

proposed as a strategy for comprehension SVM models. Before, support-vector framework loads were regularly utilized in comprehension SVM models [12]. Posthoc examination of help vector framework reenactments to characterize highlights utilized by the administrator for forecasts is a genuinely ongoing field of research exceptionally compelling in natural science.

3.3.6 CNN: Convolutional Neural Network

The expression "convolutional neural network" infers the system is using a measurable technique named convolution. Convolution is a nonstop procedure of a specific sort. Convolutional systems are basically neural systems, which use convolution in any event one of their layers rather than conventional grid duplication.
A convolutionary neural system is comprised of an info and yield layer, just as various mystery structures [14]. CNN's mystery layers, for the most part, comprise an assortment of convolutionary layers that exist together with a consequence of an increase or different dabs. The initiation work is typically a RELU sheet, which is inevitably joined by extra convolutions, for example, pooling layers, totally connected layers which standardization layers, alluded to as mystery layers as the enactment capacity and last convolution spread their sources of info and yields.
Despite the fact that the layers are called convolutions in conversational words, that is by definition as it were. It is basically a sliding point result or cross-relationship, numerically. For the lists in the network, this has significance in that it impacts how weight is determined at a given list level.

Convolutional

The info when programming a CNN is a sort tensor (picture number) x (picture width) x (picture tallness) x (picture profundity). In the wake of going by means of a convolutionary layer, the image is disconnected to a component map, with shape (number of pictures) x (highlight map width) x (include map stature) x (include map channels). A neural system convolution layer ought to have the accompanying qualities:

- Convolutionary pieces indicated by a width and tallness (hyper-parameters).
- The entirety of information channels and (hyper-parameter) yield channels.
- The Convolution channel size (the info channels) must be identical to the sum channels (width) of the information trademark plot.

Convolutional layers wind the information and move the outcome to the following line. This is undifferentiated from a neuron's response to specific boosts inside the visual cortex.[11]-convolutionary neuron produces information for its open field as it were. Albeit totally connected feedforward neural systems might be utilized to learn includes and distinguish objects, the utilization of this plan to pictures isn't reasonable. Given the wide info sizes related to photographs, where every pixel is a basic vector, an extremely high number of neurons will be required, additionally in a shallow (inverse to profound) design.

Pooling

Convolutional systems may include layers of the neighborhood or worldwide pooling to streamline the fundamental calculation. Pooling layers limit the information estimations by combining neuron bunch yields at one layer into a solitary neuron at the following layer. Nearby pooling mixes little gatherings, ordinarily 2 x 2. Worldwide pooling takes a shot at all convolutionary layer neurons. In any case, pooling will quantify a normal or a top. Max pooling utilizes the most noteworthy incentive from each bunch of the last layers of neurons. Normal pooling utilizes the normal incentive from each group of the last layer of neurons.

Fully connected

Completely connected layers tie every neuron in one layer with every neuron in another layer. In principle, it is equivalent to the regular neural perceptron multilayer (MLP) arrange. To characterize the photographs the leveled framework moves over a completely connected column.

Receptive field

Inside neural systems, each neuron gets input from an assortment of going before layer positions. Each neuron gets criticism from any piece of the former layer in a totally connected system. Neurons give criticism from just a constrained sub-territory of the former layer in a coevolutionary organize. The sub-territory is normally of a square structure (for instance, scale 5 by 5). A neuron's criticism area is called its open zone. What's more, in an entirely unexpected way.

Weights

Expanding neuron in a neural system processes a yield an incentive by adding a specific component to the info esteems in the past layer that originates from the open area. A network of loads and an inclination (commonly genuine numbers) indicates the condition which is added to the info esteems. Preparing propels by iterative changes of specific recognitions and loads in a neural system.
The weight vector and the inclination are called channels that reflect diverse information highlights (e.g., a specific shape). One distinctive trait of CNNs is that various neurons will utilize a similar channel.

CNN Architexture

A CNN design is produced by a heap of unmistakable layers that convert the volume of contribution to a volume of yield (for example keeping the class scores) by methods for a differentiable capacity. An assortment of unmistakable layer structures is generally utilized [25]. Those are recorded more underneath.

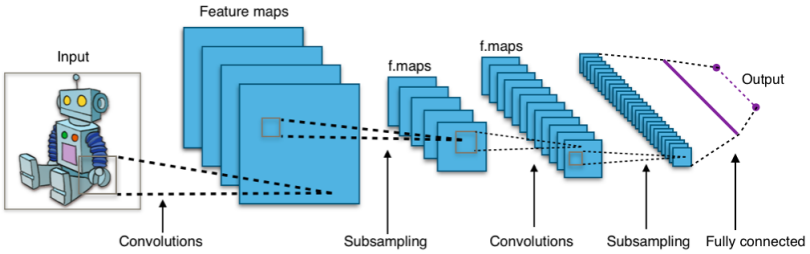

Figure 3.7: CNN Architecture

Convolutional layer
The convolutionary layer is the foundation of a CNN building. The parameters of the layer comprised of a progression of learnable channels (or pieces) with a constrained responsive territory however extending to the information volume's most extreme size. Each channel is deciphered over the width and stature of the info volume during the forward exchange, computing the speck item between the channel passages and the starting point, and creating a 2-dimensional actuation map for that channel. As a result, the system learns channels that actuate at the same spatial area in the info when it recognizes some specific type of the component.
Local connectivity
It is wasteful to interface neurons to all neurons in the past volume when managing high-dimensional information sources, for example, photographs since such a system design don't consider the spatial idea of the information. Convolutional systems expand nearby spatial closeness by forcing an inadequate example of neighborhood correspondence between neurons of neighboring layers: every neuron is connected to just a restricted territory of the volume of info.
The extent of the association is a hyperparameter called the neuron's responsive district. The interfaces are nearby in space (wide and stature long) yet regularly run over the whole width of the length of the sign.
Spatial arrangement
The size of the yield volume of the convolution layer is directed by three hyperparameters: width, stage, and zero-cushioning.

- The profundity of the volume of yield impacts the number of neurons in a layer associated with a similar information volume territory. Those neurons figure out how to trigger input for various applications. For eg, on the off chance that the first convolutionary layer accepts the crude picture as info, at that point various neurons along with the profundity measurement that triggers within the sight of explicitly coordinated edges, or shading masses.

- Stride administers how profundity segments are disseminated (width and tallness) over the spatial estimations. On the off chance that the walk is 1 so each pixel, in turn, we push the channels. This adds to the solid duplication

of open fields between segments, just as wide volumes of creation. At the point when the stage is 2 then as they move back, the channels jump 2 pixels one after another. In like manner, with on leg on each side of S permits the channel to be changed over by S units one after another per yield for each whole-number S¿0. S¿= 3 walk lengths are remarkable in sport. The open fields cover less, and where the walk span is extended, the resultant measure of yield has smaller spatial estimations.

- Often cushioning the sign with zeros at the stream volume limit is helpful. 33

Parameter sharing

In convolutionary layers, a parameter-sharing plan is utilized to deal with the number of free parameters. This is established on the reason that if a fixed work is helpful for computing at any spatial area, ascertaining at specific areas will likewise be valuable. Indicating a constant 2-dimensional cut of profundity as a cut of profundity, the neurons in each cut of profundity are compelled to utilize similar loads and predisposition.
Since all neurons in a solitary profundity cut offer similar parameters, the forward go in every profundity cut of the convolutionary layer might be estimated with the measure of contribution as a convolution of loads of the neuron. In this way, it isn't unexpected to allude to the weight sets as a channel (or part), which is changed over to the info. The result of this convolution is an initiation map, and to produce the yield number, the arrangement of actuation maps for every individual channel is stacked together along with the profundity hub. The sharing of parameters alludes to the structure of the CNN limitation invariance.
Pooling layer
Another critical idea of CNNs is pooling, which is a non-direct down-examining structure. There are a few non-direct capacities for actualizing pooling among which the most widely recognized is max pooling. It isolates the information picture into an assortment of non-covering square shapes and creates the breaking point for every one of those sub-areas.
Instinctively, the exact situation of a component, contrasted with different highlights, is less significant than its harsh position. The idea of driving the utilization of pooling in convolutionary neural systems is this. The pooling layer assists with limiting the portrayal's spatial scale gradually, to decrease the number of parameters, memory impression, and measure of calculation in the system, and in this manner to screen overfitting. It is entirely expected to intermittently embed a pooling layer between progressive convolutionary layers in a CNN architecture.[citation needed] Another kind of interpretation invariance is given by the pooling procedure.
ReLU layer
ReLU is the condensing of the redressed direct unit. By setting them to zero it basically rejects negative qualities from an enactment chart. It improves the nonlinear properties of the choice capacity and the general system, without impacting the convolution layer's open fields[23].

Fully associated layer
In the long run, the significant level deduction in the neural system is performed by means of totally connected layers, after numerous convolutionary and max-pooling layers. Neurons in a totally connected layer have a relationship in the past layer for the two actions, as found in typical (non-convolutionary) counterfeit neural systems. Consequently, their actions might be resolved as a relative change, with grid duplication joined by a balance predisposition.
Loss layer
The "misfortune layer" decides if planning punishes the distinction between the normal (yield) and genuine imprints, which is generally a neural system's last layer [6]. Different disappointment components fitting for various jobs can be utilized.

3.3.7 Confusion Matrix

Confusion Matrix might be a presentation estimation for AI characterization. it is an exhibition estimation for AI order issue where yield is frequently at least two classes. It is a table with 4 unique blends of anticipated and real qualities. It is incredibly helpful for estimating Recall, Precision, Specificity, Accuracy, and most altogether AUC-ROC Curve.

Error measurements

Four separate yield measurements are added to test the proficiency of the classifiers manufacture: False-Negative(FN) blunder, False-Positive(FP) mistake, Overall Error (OE) and Root-Mean-Square Error(RMSE). As characterized an awful smear screening is alluded to as a positive test result, and in the accompanying terms, positive cells mean unusual cells and negative cells mean ordinary cells. FN percent and FP percent are determined in conditions 1.1 and 1.2.

$$FN\% = \frac{FN}{TP + FN} \times 100\%[1.1]$$

$$FP\% = \frac{FP}{TN + FP} \times 100\%[1.2]$$

FN and FP shall signify, respectively, the number of cells misclassified as negative and positive. TN and TP are actually known as cell numbers. As mentioned earlier in section 1.3, making a FN error is more devastating than making an FP error, because patients with a pre-cancerous indication tend to be wrongly suited. In equation 1.3 the total error is defined as the number of errors relative to all the processed cells

$$OE\% = \frac{FN + FP}{TP + FN + TN + FP} \times 100\%[1.3]$$

The three previously implemented error calculations are estimation errors-a kind of numerical error figures. Since a sample is either right or incorrect-with none in between-step by step the percentage error is modified-like a separate function. The problem is defined in below example.

Example 1.1 Consider a classification of 100 samples with the following result:

TP = 67,TN = 23, FN = 5 and FP = 5. Using the definitions above the performance error is:

$$FN\% = \frac{5}{67+5} \times 100\% = 6.9\%$$

$$FP\% = \frac{5}{23+5} \times 100\% = 17.9\%$$

$$OE\% = \frac{5}{67+5+23+5} \times 100\% = 10.0\%$$

Applying the littlest potential changes to the past characterization results shows the base advance that the mistakes can change. The aggregate in the denominator in condition 1.1 and 1.2 are steady. The aggregates (TP + FN) and (T N + FP) are equivalent to the quantity of positive and negative cells in the informational index. Changing 1 example TP$\Rightarrow FNandoneexampleFP \Rightarrow TgivesTP = 67-1, FN = 5+1, TN = 23+1, andFP = 5-1$

$$FN\% = \frac{6}{66+6} \times 100\% = 8.3\%$$

$$FP\% = \frac{4}{24+4} \times 100\% = 14.86\%$$

$$OE\% = \frac{6+4}{66+6+24+4} \times 100\% = 10.0\%[1.2$$

The OE percentage is not adjusted as planned, but the FP percentage is decreased by more than 3 percent even though only one sample has improved. This means the calculations of errors are altered in measures. The size of the stage depends solely on the overall scale of the data collection and the class proportion.
Later the cross-validation is implemented to mitigate the issues with the confidence interval. The root-mean-square error(RMSE) is implemented as an alternative to the classification errors described above.

$$RMSE = \sum_{i=1}^{n} \frac{(y_i - T_i)^2}{N}[1.4]$$

RMSE is the mean difference for N samples between the classifier model output yi and the real class Ti. If the model output is integers representing the class, then the root-mean-square is equal to the square-root of the total error.
The pap-smear data is currently distributed in 7 classes but the minimum classification criteria are a question of 2 classes, discriminating between normal and abnormal cells. FN percent, FP percent, and OE percent errors of 2-class are quickly detected from a question of 7-class. As mentioned in chapter 2, class 1,2 and 3 are regular cells and irregular class 4,5,6 and 7. Figure 1.4 demonstrates the relation between a problem of two classes and a problem of seven classes.

3.3.8 AUC - ROC Curve

A collector working trademark bend, or ROC curve is a graphical plot that shows a paired classifier framework's analytic potential when the edge for segregation fluctuates.

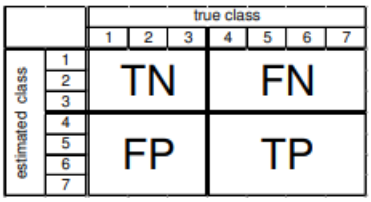

Figure 3.8: Confusion Matrices

The ROC bend is shaped by the plotting at various limit levels of the genuine positive rate (TPR) against the bogus positive rate (FPR). For AI, the genuine positive rating is frequently called responsiveness, review, or probability of recognition [27]. Otherwise called the recurrence of bogus caution is the bogus positive rate, which can be estimated as (1 explicitness). It can likewise be viewed as a forced plot because of the judgment rule's Sort I Error (when the yield is evaluated from just a single populace test, it very well may be seen as estimators of such amounts). Consequently, the ROC bend is the helplessness or review as a drop out component. When all is said in done, if the likelihood dispersions for both recognition and bogus alert are built up, the ROC bend might be made by plotting the combined conveyance capacity of the identification likelihood on the y-hub versus the aggregate dissemination capacity of the bogus caution likelihood on the x-pivot (region under the likelihood appropriation from to the separation edge).
ROC inquires about offers techniques for picking possibly ideal models and disposing of problematic models autonomously of (and before) the cost sense or class appropriation [27]. ROC inquire about is connected to cost/advantage investigate in clinical dynamic in a direct and typical way.
The ROC bend was initially produced for the distinguishing proof of unfriendly focuses in combat zones by electrical specialists and radar engineers during World War II and was then applied to brain science to make up for the visual impression of boosts. ROC examines have been utilized for a very long while in pathology, radiology, bio-metrics, cataclysmic event displaying, meteorology, a model proficiency assessment, and different fields

ROC space

The possibility table will extricate "measurements" from numerous assessments (see info-box). Just the genuine positive rate (TPR) and bogus positive rate (FPR) are required to draw a ROC bend (as elements of some classifier parameter). The TPR decides what number of the positive trials of every single substantial example that is available during the examination are precise. On the opposite side, FPR decides how frequently wrong positive results of all the incorrect examples gathered during the investigation emerge.
FPR and TPR portray a ROC space as x and y tomahawks, individually, reflecting relative exchange offs between the genuine positive (benefits) and the bogus positive (costs). Since TPR is equivalent to affectability and FPR is equivalent to 1 particularity, the plot of affectability versus (1 explicitness) is additionally called the ROC diagram. Any result or occasion of a projection of a vulnerability grid speaks to one point in the ROC space.
A point in the upper left corner or facilitate (0,1) of the ROC space will give the

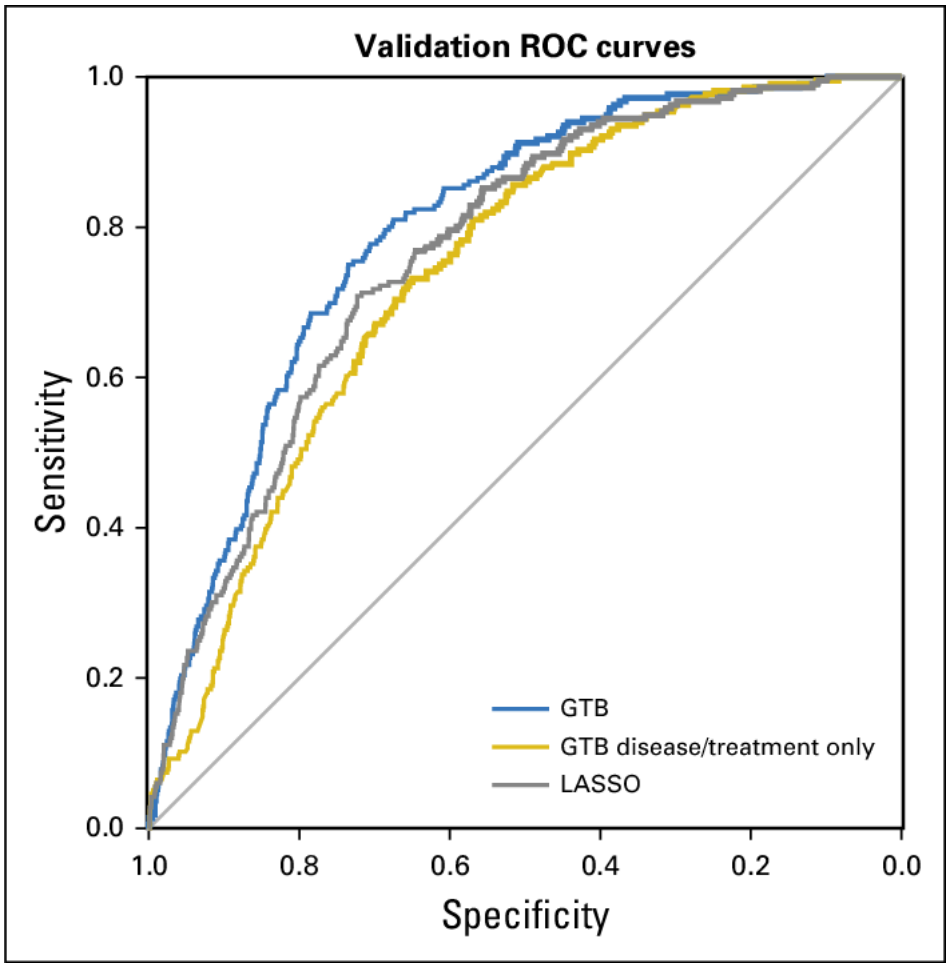

Figure 3.9: AUC-ROC Curve

most grounded conceivable forecast process, reflecting 100 percent affectability (no bogus negatives) and 100 percent precision (no bogus positives). The point (0,1) is regularly viewed as a complete positioning. An irregular conjecture will send a point from the left base to the upper right corners along with an inclining pivot (the alleged no-separation hub) (paying little mind to the positive and negative base rates). A conspicuous meaning of unconstrained wagering is flipping coins to settle on a decision. As the example size develops, the ROC-purpose of an irregular classifier focuses on the askew columns. It would prompt the level (0.5, 0.5) on account of a decent coin.
The corner to corner areas the room of the ROC. Focuses over the triangle reflect positive (superior to arbitrary) arrangement results; focuses underneath the line show poor (more regrettable than irregular) results. Notice that you may reverse the presentation of a dependably poor indicator to get a fruitful indicator.

3.4 Model Iteration

For finding out the best accuracy for detection we've used 3 types of iteration based on the number of classes of cervix cells. In the first iteration, we use 2 classes with 1 normal class which is non-cancerous and 1 abnormal class which is cancerous class. Secondly, we've taken a set of 5 classes for prediction the cell stage and in

this iteration, we've chosen 3 cancerous cervix cells and 2 non-cancerous cervix cells. Finally, in the third iteration, a set of 7 classes for cancer prediction has been chosen. In this state, we've selected 4 abnormal cancerous cells and 3 normal non-cancerous cells. In this proposed model we have done 3 iterations to check the prediction result and following a set of patterned sequences. The sequences are listed below:

- Feature Extracted Dataset
- Normalization with PCA & t-SNE
- Feature Selection using pymRMR
- Classification using SVM & XGBoost Algorithm
- Precision recall curve using AUC-ROC
- Confusion Matrix
- CNN through Inception v3

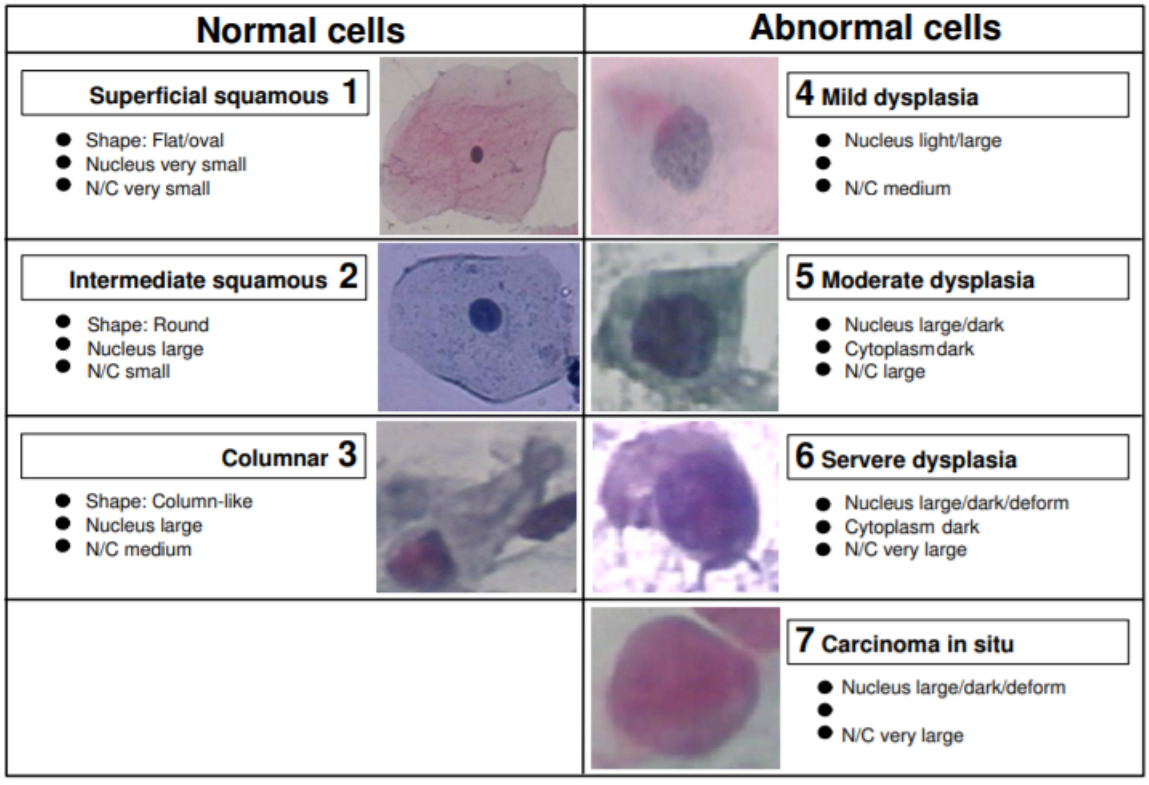

Figure 3.10: Cell type characteristics for single pap-smear cells

3.5 Feature Extraction

Feature extraction is a procedure of dimensionality decrease by which an essential game-plan of unpleasant information is diminished to intelligently sensible social events for taking care of [9]. A quality of these tremendous educational records is

endless components that require a lot of figuring advantages for process. Highlight extraction is the name for frameworks that select just as cement factors into features, sufficiently decreasing the proportion of data that must be readied, while still precisely and portraying the primary unique dataset.
The system of highlight extraction is important when you need to diminish the number of assets required for getting ready without losing noteworthy or material information. Highlight extraction can in like manner decrease the proportion of dreary information for a given examination [9]. In addition, the reduction of the data and the machine's endeavors in building variable mixes (Features) engage the speed of learning and speculation steps in the Machine Learning technique.
Since an image database that incorporates ordered pictures of single fragmented cells is put away, running it through a classifier calculation isn't quick. The cell pictures to be classified are not conventional occurrences of the 7 cell shapes but rather photos of a specific scale and direction.
These highlights among others-might be gotten from a blend of the fragmented and non-divided pictures of cells. Numerous estimations utilize just the fragmented picture, and others utilize both. A complete review of all applications can be found on page 17. Figure 3.11 offers an impression. As indicated by any pro ability, certain applications are picked. To get a full review of the structure, the rest of the highlights are picked.

1. N area(B)	8. N elongation(I)	15. C perimeter(P)
2. C area(C)	9. N roundness(J)	16. N relative position(Q)
3. N/C ratio(D)	10. C shortest diameter(K)	17. Maxima in N(R)
4. N brightness(E)	11. C longest diameter(L)	18. Minima in N(S)
5. C brightness(F)	12. C elongation(M)	19. Maxima in C(T)
6. N shortest diameter(G)	13. C roundness(N)	20. Minima in C(U)
7. N longest diameter(H)	14. N perimeter(O)	

Figure 3.11: Extracted features for pap-smear data

3.6 Building a Classifier

The reason for this benchmark information is to check and assess various arrangements. As recently revealed, the pap-smear information includes 917 examples spread in 7 gatherings and 20 characteristics distinguish each investigation. That is a fairly expansive assortment of information contrasted and a specific assortment of correlations, ex. Iris data1 From a logical perspective, it will be useful to separate between instances of mellow, moderate and extraordinary dysplasia and even in-situ Carmina-bunches 4, 5, 6 and 7, the two of which are uncommon. Classifiers checked up to this point on the information demonstrate that it is trying to recognize only between the 7 gatherings. Be that as it may, the pap-smear information might be seen as 2 class issues to decrease the order work, separating among standard and strange classes. Be that as it may, regardless of whether the last gathering is led into 2 classes, data about the seven gatherings might be utilized to oversee the model instructing.

While the conveyance is muddled, a marker of the class cover or inadequate differentiation is given by the standard deviation. At the point when the standard deviation is that, in any case, the qualification is low compared with the disparities between the class esteems. Obviously, centering at just a single alternative at once, while 20 separate highlights are accessible, is very shortsighted. A blend of numerous highlights expands the confinement better. In any case, as Martin(2003) and Byriel(1999) illustrate, the best highlights to utilize rely upon the classifier, and the assortment of working highlights builds the result of grouping. Utilizing class mean worth and standard deviation from fig 3.10, Nucleus Area(feature 1) and NC-proportion (highlight 3) are plotted against one another on figure 2.8 The standard classes 1 and 2, specifically, have all the earmarks of being distinguishable, yet the last common class 3 converges with the other odd gatherings. This means worth examination is very oversimplified, be that as it may, it offers the group habitats and class properties a clue.

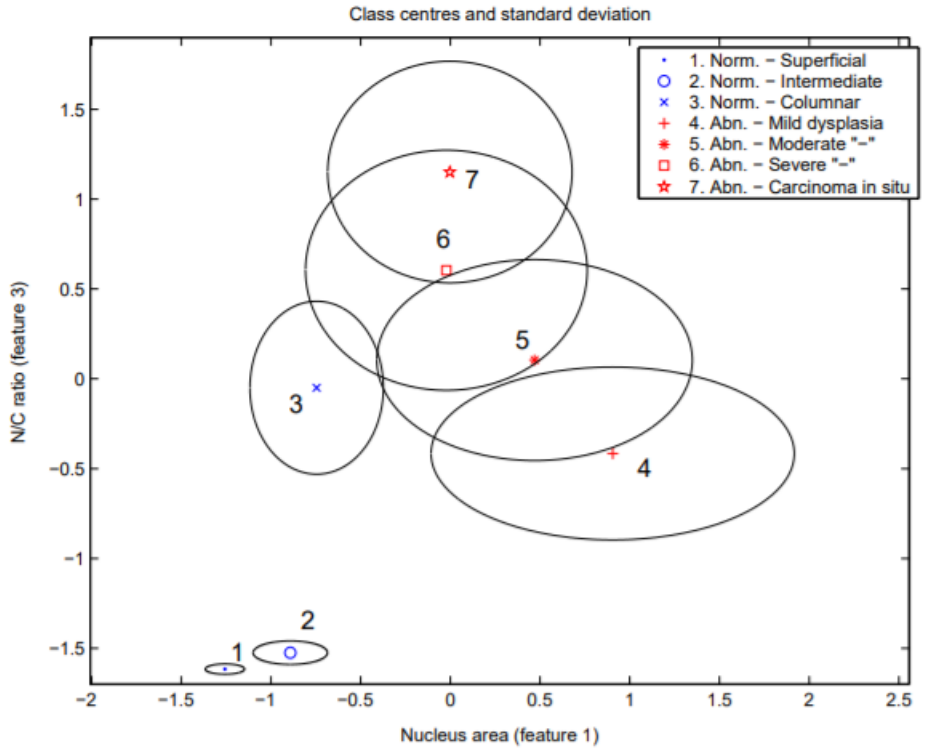

Figure 3.12: Class mean and standard deviation of pap-smear data - Nucleus Area(feature 1) and NC-ratio (feature 3)

3.7 Normalization & Standardization

Standardization and normalization words are often used interchangeably but they typically apply to specific items [24]. Normalization generally implies that a metric is standardized to have values between 0 and 1, thus standardization translates data to represent zero and normal variance 1. This standardisation is known as z-score. According to our dataset, we've used PCA(Principle Component Analysis) for normalization for feature scalling to get a better prediction[24]. Similarly, we've used

t-SNE for standardization. For both of the procedures we get two graphical graphs and those are given below:

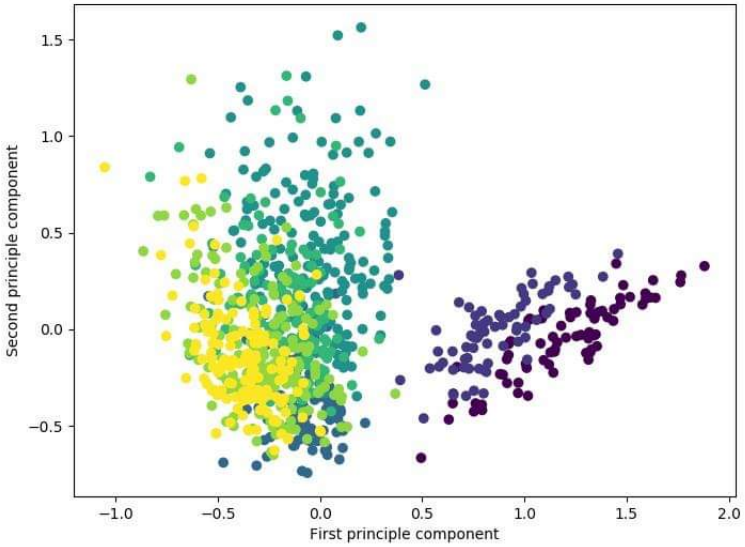

Figure 3.13: PCA Analysis Graph

Usual implementation of t-SNE conducts an internal PCA step to reduce the dimensionality of the input data to a appropriate level. Nevertheless, we are already providing PC scores as feedback we may skip this stage in either event. PCA results on PC scores contributes to similar outputs (up to the sign).

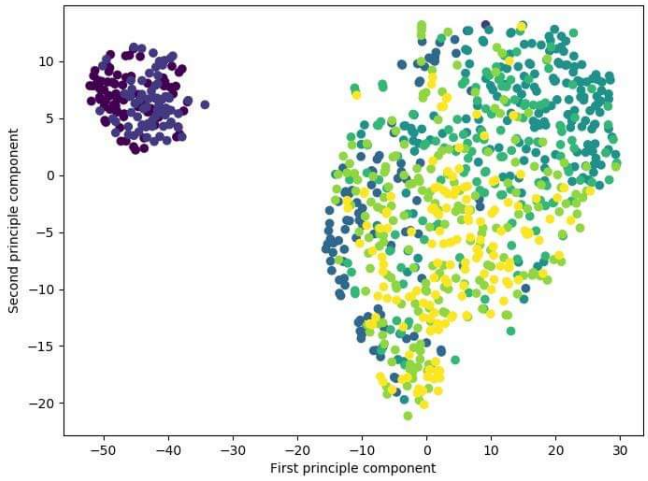

Figure 3.14: t-SNE Analysis Graph

3.8 Feature Selection Using pymRMR

TThe issue of choosing some subset of a learning calculation's information factors whereupon it should center consideration while overlooking the rest. At the end of the day, Dimensionality Reduction. In principle, the objective is to locate an ideal element subset (one that expands the scoring capacity). In genuine applications, this is normally impractical.

- For most issues, it is computationally immovable to look through the entire space of conceivable component subsets
- One, for the most part, needs to make do with approximations of the ideal subset
- Most of the exploration right now committed to finding productive hunt heuristics

Relevance of Features

There are a few meanings of pertinence in writing.

- The pertinence of 1 variable, Relevance of a variable given different factors, Relevance is given a specific learning calculation
- Most definitions are risky because there are issues where all highlights would be announced to be unimportant
- This can be characterized through two degrees of pertinence: feeble and solid importance
- A component is applicable if it is pitifully or firmly pertinent and unessential (excess) in any case.

In our examination, we've begun working with 20 highlights yet when we didn't get the necessary precision we chose to do include choice among the 20 highlights and utilizing pymRMR we've chosen 10 highlights and later we did the characterization dependent on these 10 highlights. The highlights are recorded in a figure underneath:

```
['Cyto_A',
 'CytoRund',
 'Kerne_A',
 'CytoPeri',
 'CytoMin',
 'CytoMax',
 'CytoShort',
 'KernePeri',
 'CytoLong',
 'KerneMax']
```

Figure 3.15: Feature Selection Result using pymRMR

3.9 Classification using SVM & XGBoost Algorithm

For classification, we use XGBoost for classifying with the 7 classes of our dataset. In the 7 class, we've chosen 3 normal classes of cervix cells and 4 abnormal class of cervix cells. We will do the classify using 7, 5 and 2 classes of both cancerous and non-cancerous cells. For classification, we use both XGBoost algorithms as well as SVM. In this step, we have completed 3 iterations for three types of numerical classes accordingly 2,5,7 number of classes where it consists of both the normal and abnormal cervix cells.
we get different results on two types of classification. In the SVM classifier, we get the f1 score of 0.92 and SVM classifier accuracy of 0.92 for the 2 class of cervix cells where one class is normal and another is abnormal. Similarly, we've also covered the classification for 5 and 7 classes as well. In the 5 class classification, we get the f1 score of 0.56 and for the 7 class classification, we get the f1 score of0.55.
Whereas we get a better f1 score and also the accuracy result when we did the XGBoost classification for the 7 and 5 classes. In the 5 class XGBoost, classification we get the f1 score of 0.60 and in the 7 class XGBoost classification, we get the f1score of 0.58. From the above description, we continue with the XGBoost classification model todo the CNN for prediction results. In this section, XGBoost performs better than the SVM Classification in terms of the number of classes. As the number of classes increases, we found better accuracy results for the XGBoost classification.

3.10 Precision recall curve using AUC-ROC

For a characterized question, foreseeing the likelihood of an occasion having a place with each class can be more vigorous than anticipating classes unequivocally.
This adaptability originates from the manner in which probabilities can be estimated utilizing various edges which empower the model's administrator to exchange off issues in the model's blunders, for example, the quantity of bogus positives contrasted with the quantity of bogus negatives. It is significant while using recipes where the cost of one slip-up is higher than the expense of all types of blunders.
The ROC Curves and Precision-Recall Curves are two analytic techniques that help with understanding probabilistic figures for paired (two-class) order prescient displaying issues.
There are two sorts of errors we may make when making a figure for a double or two-class grouping issue.
Genuine Positive. Anticipate an episode when it didn't occur.
Positive bogus positives. Anticipate no episode while there was a case.
By determining the chances and adjusting an edge, the model administrator will choose a blend of these two contemplations.
First of all, we might be significantly more worried about getting low bogus negatives in an exhaust cloud expectation technique than low bogus positives. A bogus negative may mean not alarm of an exhaust cloud day since it is, in actuality, a solid brown haze day, adding to open security worries that can not be tended to with measures. A bogus positive suggests that the general population may make a prudent move in the event that they hadn't.

Utilizing a ROC bend is a famous method for looking at models that foresee probabilities for two-class issues.
A capable model can give a higher probability to a specific positive occasion picked aimlessly than a negative episode by and large. That is the thing that we expect when we state there is a skill in the format. Dexterous models are typically portrayed by bends bowing up to the upper left of the chart.
A no-aptitude classifier is one that can not separate between the gatherings and in the two circumstances will figure an arbitrary class or a consistent class. At the point, a model without any capacities is seen (0.5, 0.5). At each point, a model without capacity is portrayed by an askew line from the base left of the plot to the upper right and has an AUC of 0.5.
At one phase an arrangement of incredible limit is delineated (0,1). A model of extraordinary ability is portrayed by a line running from the plot's base left to the upper left and afterward over the upper right to the middle.
An administrator can outline ROC bend for the last item and pick a limit that makes an appropriate balance between bogus positives and bogus negatives. At a point (0,1) is characterized as a result of most extreme capacity. A model of extraordinary ability is delineated by a line running from the plot's base left to the upper left and afterward over the upper right to the middle.
An administrator should delineate the last model's ROC bend, and pick an edge that gives a reasonable balance between the bogus positives and bogus negatives[1].
As referenced before, we complete having 3 cycles according to the number of classes of cervix cells. We got three accuracies versus review bends and AUC-ROC bend for our 3 sorts of cycles which comprises the number of classes. The figures of exactness versus review bends and AUC-ROC bend are given underneath:

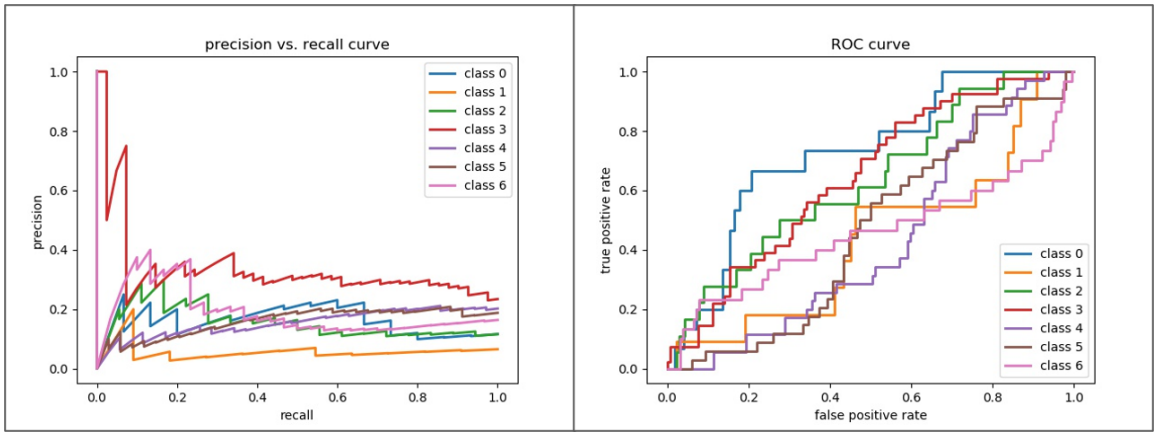

Figure 3.16: 7 Class Precision vs Recall Curve & AUC-Roc Curve

Below the figure that we are going to show represents the 5 class precision vs recall curve and AUC-ROC curve.

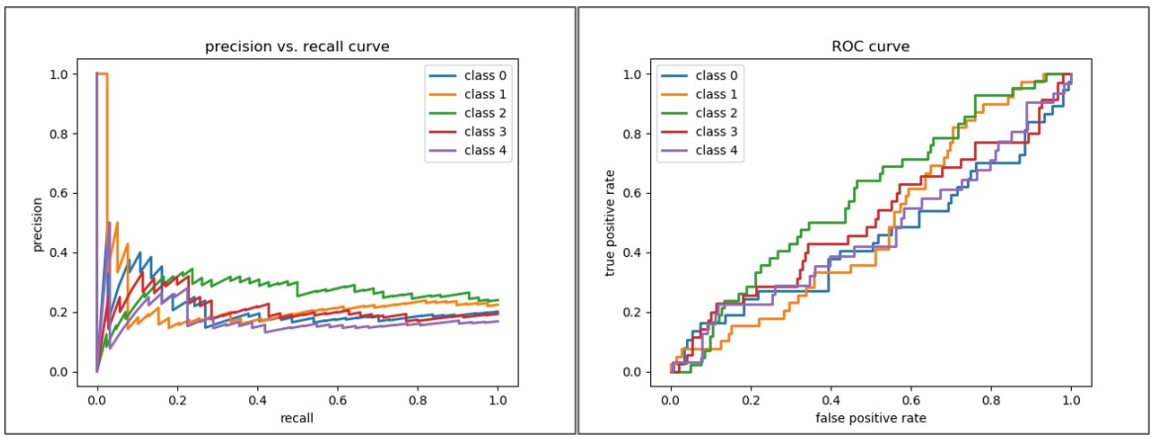

Figure 3.17: 5 Class Precision vs Recall Curve & AUC-Roc Curve

Below the figure that we are going to show represents the 2 class precision vs recall curve and AUC-ROC curve.

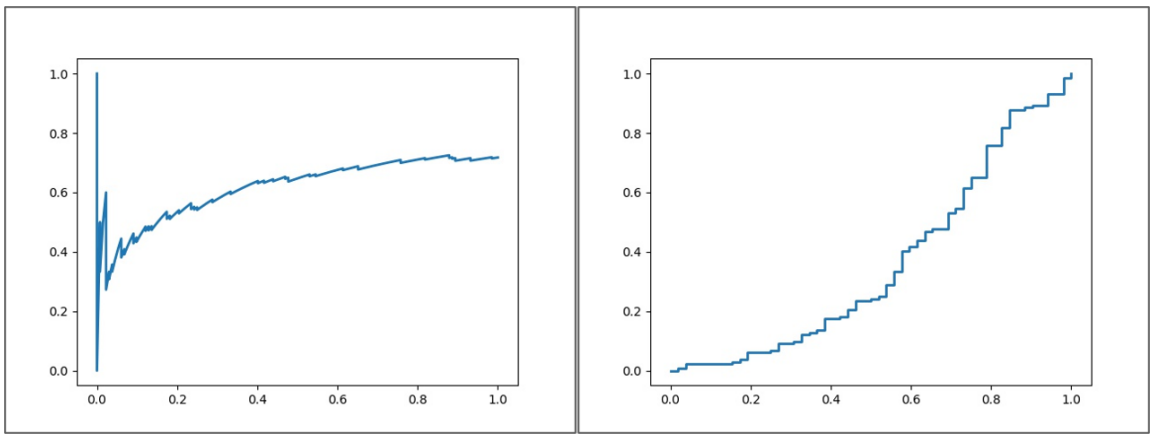

Figure 3.18: 2 Class Precision vs Recall Curve & AUC-Roc Curve

3.11 Confusion Matrix

At the point when we have the outcomes, the initial step we do after outcomes washing, pre-preparing and wrangling are to take care of it to a great model and have yielded in probability. Yet, simply keep things under control! How in the hellfire we will ascertain our model's viability [2]. More excellent, better outcomes, and we need that precisely. So this is the place the structure of Confusion comes back to the spotlight. Disarray Matrix is a measurement of accomplishment for grouping AI.

The fundamental issue with order exactness is that it disguises the data you have to all the more likely comprehend your arrangement model's outcomes. There are two models where this inquiry is well on the way to happen:

- If the information has multiple levels. You may get an 80 percent arrangement accuracy for at least 3 classes, yet you don't realize whether that is because

the two classes are normal genuinely well or whether the model disregards a couple of classes

- Then there are no even quantities of classes in your outcomes. You can arrive at 90 percent or more exactness, yet that is certifiably not a sensible score if 90 records for every 100 have a place with one class and you will just accomplish that score anticipating the most well-known class esteem.

At that point, such numbers are masterminded into a rundown, or a framework as follows: Projected drawback: each line of the lattice connects to a class foreseen [2]. Anticipated over the top: Every network segment associates to a real class. The good and bad portrayal includes are then filled in into the table. The aggregate measure of right class forecasts goes into the arranged line for that class esteem and the anticipated class esteem section.
Moreover, with each class esteem, the combined measure of off base forecasts for a class falls into the arranged line and for that class esteem, the anticipated section falls. This recipe can be utilized for 2-class issues where it is exceptionally straightforward yet can be effortlessly applied to issues with at least 3 class qualities, by acquainting extra lines and sections with the vulnerability condition.
Two-class Problems Are Unique In a two-class issue, we likewise attempt to recognize, from regular perceptions, between perceptions with a specific result. These as the condition or instances of confusion from no kind of ailment or event.
What's more, we ought to distribute the episode line to be "solid" and the no-occasion line to be "negative." So we may add gauges to the occasion section as "genuine," and no-occasion as "fiction."
This brings us:
Since we've been going on an essential contextual investigation of the 2-class disarray framework, we should perceive how we may gauge a disarray lattice with current profound learning programming.

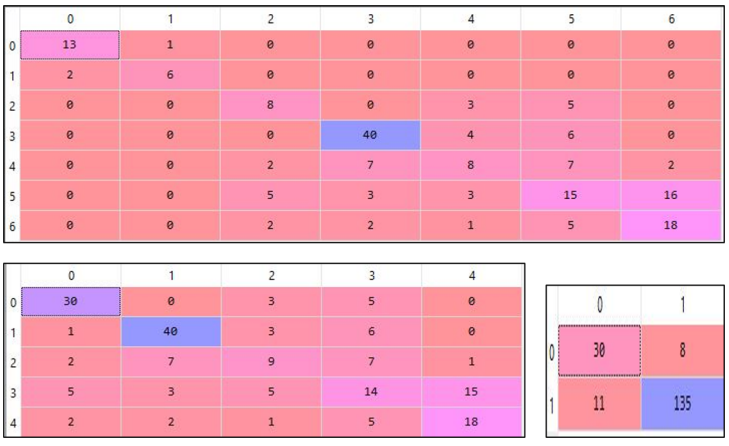

Figure 3.19: Confusion Matrix Result of 2, 5, 7 Classes of Cervix Cell

3.12 CNN through Inception v3

Artificial intelligence and neural networks also taken the analysis of pictures to a whole new stage. Processes which used to take days or weeks can be carried out in a matter of hours now. But some creative people, including developers from Apriorit, are moving much deeper and searching for ways to use neural networks that were initially designed for image recognition to solve tasks related to video analysis and classification.
A convolutional neural network (CNN) is a counterfeit neural system engineering that intends to perceive designs [14]. In 2012, when a CNN empowered Alex Krizhevsky, the organizer of AlexNet, to win the ImageNet Large Scale Visual Recognition Challenge (ILSVRC) by hitting the best 5 mistake pace of 15.3 percent, CNNs got wide acknowledgment inside the innovation gathering.
A couple of years after the fact, Google made its CNN named GoogleNet, otherwise called Inception V1, which turned into the 2014 ILSVRC champion with a 6.67 percent top-5 blunder rate. From that point, the example was improved and refreshed commonly[19]. Four emphases of the neural system Development happen to start today. Commencement V3 is regularly utilized with a pretrained profound neural system for picture acknowledgment. All through this article, we investigate utilizing this CNN to address video arrangement issues, utilizing, as a representation, a clasp of a football affiliation communicates.
Through acquainting new information bunches with a pre-prepared Inception V3 model Pass gaining from Inception V3, the current neural system can be retrained to utilize it to illuminate custom picture order undertakings [14]. We may utilize the TensorFlow-picture classifier vault to join new kinds of information to the pretrained Inception V3 design. This storehouse incorporates a progression of contents for introducing and retraining the default release of the Inception V3 model for the characterization of another age of photographs utilizing Python 3, Tensorflow and Keras.
Since it doesn't take much time to attach new data groups to the current neural network, you can run all of the programming processes either on your own computer or in Google CoLab.
Let's go on to the Inception V3 retraining phase for classifying new details. In our example below we train our model in several photos to identify the face of cerrvix cells images. To retrain the neural network we need a dataset of photos that are categorized. In our scenario, we use this dataset of 1,000 photos of the cervix cells images where we divide it into 7 class types.
Next, we need to build a training dataset folder with all the photos divided by the names of the cervix image into 2 subfolders: Normal Abnormal cervix cells. In a cloned tensorflow-image-classifier library, thus, we have the following file structure:
Then we remove two photographs (as test data) from each sub-folder that holds the pictures of the athletes and transfer them to the folder of the tensor flow-image-classifier so that they will not be required for training. Now all is ready for our Iteration V3 platform to be retrained.
The./train.sh script loads the already qualified Inception V3 construct, deletes the upper layer and then trains a new layer on the data groups we've installed with photos of the cervix cells of normal and abnormal classes. The whole cycle of retraining the model consists of two stages:

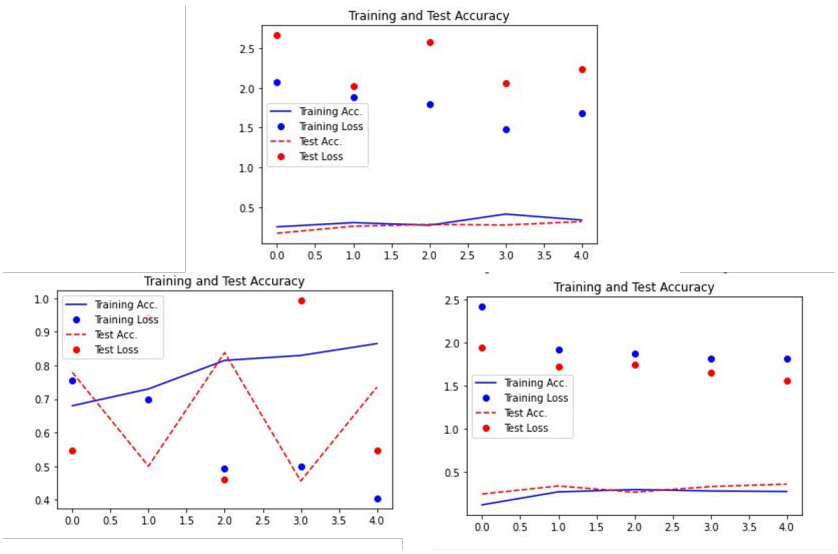

Figure 3.20: CNN Inception v3 Test & Training Result of 2, 5, 7 Classes of Cervix Cell

- The script analyzes all the artifacts on the disk at the first point and determines the bottleneck values for each of them. "Bottleneck" is a non-official phrase used for the layer that occurs just below the final layer of production that really executes the classification. As a result of this point, we get a concise type of definition of the picture which makes the classification run far quicker. We're thinking about the weights for a particular layer within the sense of the Inception model.

- In the second level, we pass on to the network's real upper layer preparation. You will see a sequence of preparation measures here, each of which demonstrates the degree of consistency of the testing and cross entropy. The consistency of the instruction indicates the number of instruction photos that were accurately identified. Cross entropy is a loss function which shows the training process performance. Cross entropy also serves as a symbol of a configuration that is under trained or over trained.

Chapter 4

Result & Analysis

4.1 Benchmark database

The present assortment of pap-smear information from Herlev University Hospital is recorded in section 2 of a restricted reference control. Each archive gives an autonomous review of all parts of the sources of info and the 7 explicit levels.
The guide is implied as an enhancement to the present pap-smear assortment with inferred highlights contained on the encased CD-ROM in Appendix A. The point is to present all free-on use subtleties on the WWW as a correlation. A classifier might be checked essentially by transferring the Excel-data sheet, yet class and capacity subtleties might be helpful eg. Decrease to a disentangled inquiry of 2 levels or decrease of capacities. Like other examination informational indexes, the pap-smear assortment is differing with different tests, numerous traits, and a few separate evaluations. However, there will need to be more rearrangements. The vulnerability grid in table 3.3 on page 33 demonstrates from the Least Squared gathering into 7 unique gatherings that moving all class 3 examples will permit a qualification among normal and unpredictable cells far more straightforward. Taking a gander at the line of class 3 and the segment of class 3, it uncovers that many class 3 examples are misclassified as unpredictable (class 4,567) and other anomalous cells are misclassified as tests of class 3. The point of distributing the pap-smear on the World Wide Web is to grow the consciousness of the database and in a perfect world get improved classifiers over the long haul. That will help Herlev University Hospital and the logical field of pap-smear as a rule. Electronic programming might be worked with benefits to raise the prominence of the website and get more taps on the World Wide Web.

4.2 Classification Results

Various forms of classifiers were evaluated on the pap-smear data to boost earlier performance. They were basically divided into:

- SVM: Support Vector Machine
- XGBoost Algorithm

Owing to a pointless classification error of more than 40%, direct grouping into the 7 unique classes in the pap-smear database was practically unimaginable. In

any case, the examination indicated that a depiction of the scalar class was not adequate for grouping in multiple classes. Nevertheless, there was no optimization of the 6 threshold rates. And the modification of these thresholds will most likely increase the classification error[8]. More square fitting may be used to maximize the 6 threshold stage. It will add new weight and the best outcomes are possibly the same as the binary class solution.
we get different results on two types of classification. In the SVM classifier we get the f1 score of 0.92 and SVM classifier accuracy of 0.92 for the 2 class of cervix cell where one class is normal and another is abnormal. In the similar way we've also covered the classification for 5 and 7 classes as well. In the 5 class classification we get the f1 score of 0.56 and for the 7 class classification we get the f1 score of 0.55.

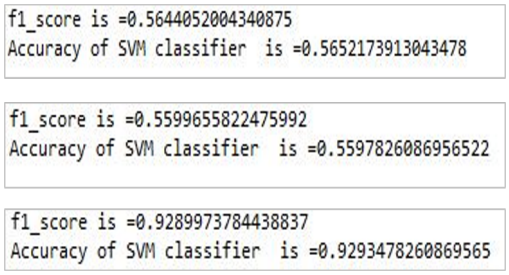

Figure 4.1: F1 Score & Accuracy Result of 2, 5, 7 Classes of Cervix Cell for SVM Classification

Whereas we get better f1 score and also the accuracy result when we did the XG-Boost classification for the 7 and 5 class. In the 5 class XGBoost classification we get the f1 score of 0.60 and in the 7 class XGBoost classification we get the f1 score of 0.58.

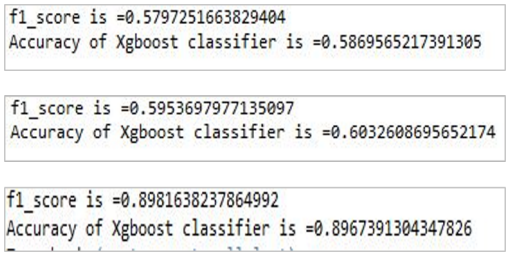

Figure 4.2: F1 Score & Accuracy Result of 2, 5, 7 Classes of Cervix Cell for XGBoost Classification

4.3 CNN Inception v3 Result Analysis

Let's go on to the Inception V3 retraining phase for classifying new details. In our example below we train our model in several photos to identify the face of cerrvix cells images [29]. To retrain the neural network we need a dataset of photos that are categorized. In our scenario, we use this dataset of 1,000 photos of the cervix cells images where we divide it into 7 class types.
Next, we need to build a training dataset folder with all the photos divided by the names of the cervix image into 2 subfolders: Normal Abnormal cervix cells. In a cloned tensorflow-image-classifier library, thus, we have the following file structure:

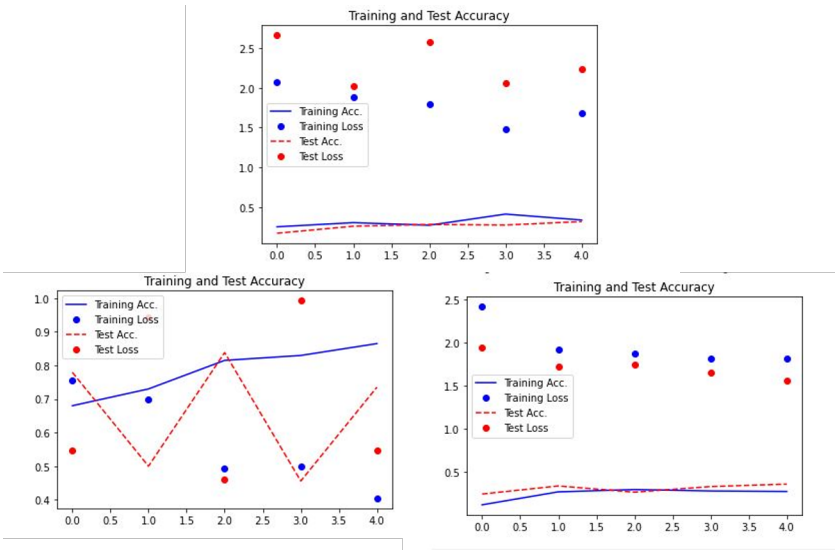

Figure 4.3: CNN Inception v3 Test & Training Result of 2, 5, 7 Classes of Cervix Cell

Our classification model's final check performance is 86.1 percent. Considering the amount of photos in the dataset this result is strong. The degree of precision of the training will be improved if we increase the amount of photos used to train the pattern[4].
The product of running the ./train.sh script looks like this:

```
Epoch 1/5
 9/10 [==========================>...] - ETA: 0s - loss: 1.6151 - categorical_accuracy: 0.3833Epoch 1/5
10/10 [==============================] - 7s 717ms/step - loss: 1.6236 - categorical_accuracy: 0.3800 - val_loss: 2.1826 - val_categorical_accuracy: 0.3235
Epoch 2/5
 9/10 [==========================>...] - ETA: 0s - loss: 1.6030 - categorical_accuracy: 0.4056Epoch 1/5
10/10 [==============================] - 7s 682ms/step - loss: 1.5975 - categorical_accuracy: 0.3950 - val_loss: 1.7732 - val_categorical_accuracy: 0.3529
Epoch 3/5
 9/10 [==========================>...] - ETA: 0s - loss: 1.4569 - categorical_accuracy: 0.4000Epoch 1/5
10/10 [==============================] - 6s 646ms/step - loss: 1.4277 - categorical_accuracy: 0.4011 - val_loss: 1.8672 - val_categorical_accuracy: 0.3897
Epoch 4/5
 9/10 [==========================>...] - ETA: 0s - loss: 1.4618 - categorical_accuracy: 0.4222Epoch 1/5
10/10 [==============================] - 7s 678ms/step - loss: 1.4676 - categorical_accuracy: 0.4150 - val_loss: 1.7902 - val_categorical_accuracy: 0.3971
Epoch 5/5
 9/10 [==========================>...] - ETA: 0s - loss: 1.3705 - categorical_accuracy: 0.4111Epoch 1/5
10/10 [==============================] - 7s 652ms/step - loss: 1.3101 - categorical_accuracy: 0.4176 - val_loss: 1.8160 - val_categorical_accuracy: 0.4044
```

```
Epoch 1/5
 9/10 [==========================>...] - ETA: 0s - loss: 1.7425 - categorical_accuracy: 0.3278Epoch 1/5
10/10 [==============================] - 7s 684ms/step - loss: 1.8211 - categorical_accuracy: 0.3242 - val_loss: 1.7703 - val_categorical_accuracy: 0.3309
Epoch 2/5
 9/10 [==========================>...] - ETA: 0s - loss: 1.7426 - categorical_accuracy: 0.3333Epoch 1/5
10/10 [==============================] - 7s 684ms/step - loss: 1.6930 - categorical_accuracy: 0.3550 - val_loss: 1.7267 - val_categorical_accuracy: 0.3022
Epoch 3/5
 9/10 [==========================>...] - ETA: 0s - loss: 1.5191 - categorical_accuracy: 0.3944Epoch 1/5
10/10 [==============================] - 7s 676ms/step - loss: 1.5115 - categorical_accuracy: 0.4050 - val_loss: 1.7585 - val_categorical_accuracy: 0.2806
Epoch 4/5
 9/10 [==========================>...] - ETA: 0s - loss: 1.4001 - categorical_accuracy: 0.4611Epoch 1/5
10/10 [==============================] - 7s 682ms/step - loss: 1.3909 - categorical_accuracy: 0.4600 - val_loss: 1.7535 - val_categorical_accuracy: 0.2878
Epoch 5/5
 9/10 [==========================>...] - ETA: 0s - loss: 1.4766 - categorical_accuracy: 0.4222Epoch 1/5
10/10 [==============================] - 7s 677ms/step - loss: 1.4690 - categorical_accuracy: 0.4250 - val_loss: 1.6006 - val_categorical_accuracy: 0.3597
```

```
Epoch 1/5
 9/10 [==========================>...] - ETA: 4s - loss: 0.7711 - categorical_accuracy: 0.6833Epoch 1/5
10/10 [==============================] - 45s 4s/step - loss: 0.7555 - categorical_accuracy: 0.6800 - val_loss: 0.5483 - val_categorical_accuracy: 0.7794
Epoch 2/5
 9/10 [==========================>...] - ETA: 0s - loss: 0.6952 - categorical_accuracy: 0.7444Epoch 1/5
10/10 [==============================] - 7s 672ms/step - loss: 0.6985 - categorical_accuracy: 0.7300 - val_loss: 0.9428 - val_categorical_accuracy: 0.5000
Epoch 3/5
 9/10 [==========================>...] - ETA: 0s - loss: 0.5418 - categorical_accuracy: 0.7944Epoch 1/5
10/10 [==============================] - 7s 663ms/step - loss: 0.4946 - categorical_accuracy: 0.8150 - val_loss: 0.4604 - val_categorical_accuracy: 0.8382
Epoch 4/5
 9/10 [==========================>...] - ETA: 0s - loss: 0.4533 - categorical_accuracy: 0.8272Epoch 1/5
10/10 [==============================] - 8s 822ms/step - loss: 0.4641 - categorical_accuracy: 0.8297 - val_loss: 0.9929 - val_categorical_accuracy: 0.4559
Epoch 5/5
 9/10 [==========================>...] - ETA: 0s - loss: 0.4275 - categorical_accuracy: 0.8611Epoch 1/5
10/10 [==============================] - 7s 677ms/step - loss: 0.4042 - categorical_accuracy: 0.8650 - val_loss: 0.5483 - val_categorical_accuracy: 0.7353
```

Figure 4.4: Categorical Accuracy Result of 2, 5, 7 Classes of Cervix Cell

Chapter 5

Conclusion & Future Plan

Cervical malignancy is a disease that has its foundations in the cervix. This is because of the unusual improvement of cells fit for arriving at specific pieces of the body or spreading to them. There are generally no side effects seen at an early stage. Later side effects can incorporate unreasonable vaginal dying, stomach torment, or sickness during sex; Although there may not be any huge after-sex dying, it might likewise show cervical malignant growth.
Contamination with human papillomavirus (HPV) influences in excess of 90 percent of cases, however, the vast majority with HPV diseases don't create cervical malignant growth [5]. Liquor, a frail invulnerable framework, contraception pills, starting pubescence at a youthful age and having numerous sexual accomplices are other hazard factors, yet they are less significant.
Cervical malignant growth regularly becomes more than 10 to 20 years from precancerous modifications. Roughly 90 percent of instances of a cervical malignant growth are squamous cell carcinomas, 10 percent are adenocarcinoma and different structures are a modest number. By and large, the conclusion incorporates cervical screening joined by biopsy. Regularly, clinical testing is performed to survey whether malignant growth has progressed or has not.
A complete, independent rundown has been given from a setup database of single pap-smear cells with 20 highlights previously extricated. Utilizing the database, a fundamental worksheet with highlights and class definition along with the segments and tests at the edges, and it is conceivable to check own classifiers on the information utilizing the made guide.

5.1 Future Plan

At this point of our research on cervical cancer detection is limited to CNN(Convolutional Neural Network). In future we are explicitly enthusiast to add a new detection model that is DBN(Deep Belief Network) [10]. A Deep Belief Network (DBN) in AI is a generative realistic model, or rather a sort of profound neural system, comprising of a few layers of inert factors ("concealed units"), with associations between layers yet not between units inside each layer[10].
At the point when prepared without direction on an assortment of examples, a DBN can figure out how to reproduce its contributions to a probabilistic way. The layers then serve as detectors for apps. Following this learning stage a DBN may be further taught to conduct classification with supervision. Currently we are getting

70 percent of accuracy in terms of 7 class detection which carries 4 abnormal and 3 normal cervix cell and we are keen to get the highest accuracy possible above 90 percent.

Bibliography

[1] T. Kanungo, D. M. Gay, and R. M. Haralick, "Constrained monotone regression of roc curves and histograms using splines and polynomials", in *Proceedings., International Conference on Image Processing*, vol. 2, 1995, 292–295 vol.2.

[2] L. Chen and H. L. Tang, "Improved computation of beliefs based on confusion matrix for combining multiple classifiers", *Electronics Letters*, vol. 40, no. 4, pp. 238–239, 2004.

[3] K. A. Kumar, A. K. Pappu, K. S. Kumar, and S. Sanyal, "Hybrid approach for parallelization of sequential code with function level and block level parallelization", in *International Symposium on Parallel Computing in Electrical Engineering (PARELEC'06)*, 2006, pp. 161–166.

[4] A. Mathur and G. M. Foody, "Multiclass and binary svm classification: Implications for training and classification users", *IEEE Geoscience and Remote Sensing Letters*, vol. 5, no. 2, pp. 241–245, 2008.

[5] S. Chen, K. Lin, C. Tang, S. Peng, Y. Chuang, Y. Lin, J. Wang, and C. Lin, "Optical detection of human papillomavirus type 16 and type 18 by sequence sandwich hybridization with oligonucleotide-functionalized au nanoparticles", *IEEE Transactions on NanoBioscience*, vol. 8, no. 2, pp. 120–131, 2009.

[6] N. Feng and Y. Jianming, "Line losses calculation in distribution network based on rbf neural network optimized by hierarchical ga", in *2009 International Conference on Sustainable Power Generation and Supply*, 2009, pp. 1–5.

[7] Y. Yang, P. Liu, Z. Zhu, and Y. Qiu, "The research of an improved information gain method using distribution information of terms", in *2009 IEEE International Symposium on IT in Medicine Education*, vol. 1, 2009, pp. 938–941.

[8] T. Haumtratz, J. Worms, and J. Schiller, "Classification of air targets including a rejection stage for unknown targets", in *11-th INTERNATIONAL RADAR SYMPOSIUM*, 2010, pp. 1–4.

[9] S. Ansari and U. Sutar, "Optimized and efficient feature extraction method for devanagari handwritten character recognition", in *2015 International Conference on Information Processing (ICIP)*, 2015, pp. 11–15.

[10] Yuming Hua, Junhai Guo, and Hua Zhao, "Deep belief networks and deep learning", in *Proceedings of 2015 International Conference on Intelligent Computing and Internet of Things*, 2015, pp. 1–4.

[11] A. J. Zaylaa, A. Harb, F. I. Khatib, Z. Nahas, and F. N. Karameh, "Entropy complexity analysis of electroencephalographic signals during pre-ictal, seizure and post-ictal brain events", in *2015 International Conference on Advances in Biomedical Engineering (ICABME)*, 2015, pp. 134–137.

[12] R. Chen and Y. Wang, "A study of the weighted least squares support vector machine within the bayesian evidence framework", in *2016 IEEE International Conference on Aircraft Utility Systems (AUS)*, 2016, pp. 616–619.

[13] F. R. On, R. Jailani, S. L. Hassan, and N. M. Tahir, "Analysis of sparse pca using high dimensional data", in *2016 IEEE 12th International Colloquium on Signal Processing Its Applications (CSPA)*, 2016, pp. 340–345.

[14] S. Albawi, T. A. Mohammed, and S. Al-Zawi, "Understanding of a convolutional neural network", in *2017 International Conference on Engineering and Technology (ICET)*, 2017, pp. 1–6.

[15] A. Albayrak, A. Ünlü, N. Çalık, G. Bilgin, İ. Türkmen, A. Çakır, A. Çapar, B. U. Töreyin, and L. D. Ata, "Segmentation of precursor lesions in cervical cancer using convolutional neural networks", in *2017 25th Signal Processing and Communications Applications Conference (SIU)*, 2017, pp. 1–4.

[16] M. R. Hasan, H. Gholamhosseini, N. I. Sarkar, and S. M. Safiuzzaman, "Intrinsic motivated cervical cancer screening intervention framework", in *2017 IEEE Region 10 Humanitarian Technology Conference (R10-HTC)*, 2017, pp. 506–509.

[17] R. Sinha and J. Clarke, "When technology meets technology: Retrained 'inception v3' classifier for ngs based pathogen detection", in *2017 IEEE International Conference on Bioinformatics and Biomedicine (BIBM)*, 2017, pp. 1–5.

[18] M. Yu, S. Zhang, L. Zhao, and G. Kuang, "Deep supervised t-sne for sar target recognition", in *2017 2nd International Conference on Frontiers of Sensors Technologies (ICFST)*, 2017, pp. 265–269.

[19] Z. Zhu, J. Li, L. Zhuo, and J. Zhang, "Extreme weather recognition using a novel fine-tuning strategy and optimized googlenet", in *2017 International Conference on Digital Image Computing: Techniques and Applications (DICTA)*, 2017, pp. 1–7.

[20] A. A. Almisreb, N. Jamil, and N. M. Din, "Utilizing alexnet deep transfer learning for ear recognition", in *2018 Fourth International Conference on Information Retrieval and Knowledge Management (CAMP)*, 2018, pp. 1–5.

[21] L. Jidong and Z. Ran, "Dynamic weighting multi factor stock selection strategy based on xgboost machine learning algorithm", in *2018 IEEE International Conference of Safety Produce Informatization (IICSPI)*, 2018, pp. 868–872.

[22] V. Partanen, M. Pankakoski, Z. Bzhalava, P. Veerus, A. Anttila, T. Sarkeala, A. Tropé, S. Lönnberg, S. Heinävaara, J. Dillner, and Á. I. Ágústsson, "Nordscreen - an interactive tool for presenting cervical cancer screening indicators in the nordic countries", in *2018 IEEE 14th International Conference on e-Science (e-Science)*, 2018, pp. 287–287.

[23] J. Si, S. L. Harris, and E. Yfantis, "A dynamic relu on neural network", in *2018 IEEE 13th Dallas Circuits and Systems Conference (DCAS)*, 2018, pp. 1–6.

[24] A. N. Abbasi and M. He, "Convolutional neural network with pca and batch normalization for hyperspectral image classification", in *IGARSS 2019 - 2019 IEEE International Geoscience and Remote Sensing Symposium*, 2019, pp. 959–962.

[25] X. Han, Y. Sun, and Y. Chen, "Residual component estimating cnn for image super-resolution", in *2019 IEEE Fifth International Conference on Multimedia Big Data (BigMM)*, 2019, pp. 443–447.

[26] A. Jain, A. A. Awan, H. Subramoni, and D. K. Panda, "Scaling tensorflow, pytorch, and mxnet using mvapich2 for high-performance deep learning on frontera", in *2019 IEEE/ACM Third Workshop on Deep Learning on Supercomputers (DLS)*, 2019, pp. 76–83.

[27] P. Pourmohammadi, D. Adjeroh, and M. P. Strager, "Predicting impervious land expansion using deep deconvolutional neural networks", in *IGARSS 2019 - 2019 IEEE International Geoscience and Remote Sensing Symposium*, 2019, pp. 9855–9858.

[28] W. WILLIAM, A. WARE, A. H. BASAZA-EJIRI, and J. OBUNGOLOCH, "Automated diagnosis and classification of cervical cancer from pap-smear images", in *2019 IST-Africa Week Conference (IST-Africa)*, 2019, pp. 1–11.

[29] G. Zheng, G. Han, and N. Q. Soomro, "An inception module cnn classifiers fusion method on pulmonary nodule diagnosis by signs", *Tsinghua Science and Technology*, vol. 25, no. 3, pp. 368–383, 2020.